Mitochondrial fission facilitates the selective mitophagy of protein aggregates

Jonathon L. Burman,[1] Sarah Pickles,[1] Chunxin Wang,[1] Shiori Sekine,[1] Jose Norberto S. Vargas,[1] Zhe Zhang,[1] Alice M. Youle,[2] Catherine L. Nezich,[1] Xufeng Wu,[2] John A. Hammer,[2] and Richard J. Youle[1]

[1]Biochemistry Section, Surgical Neurology Branch, National Institute of Neurological Disorders and Stroke and [2]Molecular Cell Biology Section, National Heart, Lung, and Blood Institute, National Institutes of Health, Bethesda, MD

Within the mitochondrial matrix, protein aggregation activates the mitochondrial unfolded protein response and PINK1–Parkin-mediated mitophagy to mitigate proteotoxicity. We explore how autophagy eliminates protein aggregates from within mitochondria and the role of mitochondrial fission in mitophagy. We show that PINK1 recruits Parkin onto mitochondrial subdomains after actinonin-induced mitochondrial proteotoxicity and that PINK1 recruits Parkin proximal to focal misfolded aggregates of the mitochondrial-localized mutant ornithine transcarbamylase (ΔOTC). Parkin colocalizes on polarized mitochondria harboring misfolded proteins in foci with ubiquitin, optineurin, and LC3. Although inhibiting Drp1-mediated mitochondrial fission suppresses the segregation of mitochondrial subdomains containing ΔOTC, it does not decrease the rate of ΔOTC clearance. Instead, loss of Drp1 enhances the recruitment of Parkin to fused mitochondrial networks and the rate of mitophagy as well as decreases the selectivity for ΔOTC during mitophagy. These results are consistent with a new model that, instead of promoting mitophagy, fission protects healthy mitochondrial domains from elimination by unchecked PINK1–Parkin activity.

Introduction

Parkin is an E3 ubiquitin ligase that functions downstream of PINK1 in a pathway capable of identifying and eliminating dysfunctional mitochondria (Pickrell and Youle, 2015). After mitochondrial damage, PINK1 accumulates on the outer mitochondrial membrane, where it phosphorylates polyubiquitin chains linked to mitochondrial outer membrane proteins. Phospho-S65-ubiquitin binds to Parkin, recruiting it from the cytosol and activating Parkin's E3 ubiquitin ligase activity. Parkin activation induces further ubiquitination of mitochondrial outer membrane proteins, in turn generating more ubiquitin substrate for PINK1, yielding a potent feedback amplification circuit. Phosphoubiquitin chains on outer mitochondrial membrane proteins recruit autophagy receptors, which recruit upstream autophagy machinery and induce the selective autophagy of damaged mitochondria (Lazarou et al., 2015).

Mitochondrial fission depends on the function of the dynamin family GTPase Drp1 (Friedman and Nunnari, 2014). Drp1-mediated fission has been thought to facilitate mitophagy by dividing mitochondria into fragments amenable to autophagosome engulfment (Tanaka et al., 2010; Gomes et al., 2011; Rambold et al., 2011) and/or segregating damaged mitochondrial subdomains for elimination (Twig et al., 2008). Additionally, Drp1 overexpression compensates for a loss of PINK1 or Parkin in *Drosophila melanogaster*, genetically linking PINK1 and Parkin to mitochondrial fission (Deng et al., 2008; Poole et al., 2008; Burman et al., 2012). However, other studies indicate that Drp1 is not required for mitophagy (Mendl et al., 2011; Song et al., 2015; Yamashita et al., 2016).

Although several mitochondrial stresses that promote Parkin recruitment are associated with membrane depolarization (Youle and van der Bliek, 2012), misfolded protein expression is capable of recruiting Parkin to mitochondria without depolarizing the inner mitochondrial membrane, and it may represent a more physiological mechanism of PINK1 stabilization (Jin and Youle, 2013). Although quantitative mass spectrometry research shows that PINK1–Parkin can mediate selective turnover of mitochondrial matrix substrates via autophagy (Vincow et al., 2013), how Parkin can selectively eliminate mitochondrial matrix–localized misfolded protein via autophagy remains unknown. In this study, we show that cytosolic Parkin is recruited by PINK1 to focal spots on mitochondria that are proximal to ornithine transcarbamylase (OTC) lacking amino acids 30–114 (ΔOTC) aggregates within the mitochondrial matrix. Although the formation of Parkin foci correlates with Drp1-mediated fission, we find that Drp1 is not required for mitophagy. Unexpectedly, Drp1 knockout (KO) cells display constitutive recruitment of Parkin to elongated mitochondrial networks and increased rates of steady-state mitophagy. We propose the new

Correspondence to Richard J. Youle: youler@ninds.nih.gov

Abbreviations used: KO, knockout; MDV, mitochondrial-derived vesicle; mtDNA, mitochondrial DNA; OA, oligomycin/antimycin A; OTC, ornithine transcarbamylase; PDH, pyruvate dehydrogenase; RACE, rapid amplification of cDNA ends; TMRM, tetramethylrhodamine, methyl ester.

The Rockefeller University Press
J. Cell Biol. Vol. 216 No. 10 3231–3247
https://doi.org/10.1083/jcb.201612106

model that Drp1-mediated mitochondrial fission is required not to facilitate efficient mitophagy of mitochondrial fragments, but to spare the healthy mitochondrial subdomains from unchecked PINK1–Parkin activity. Thus, mitochondrial fission is proposed to break the PINK1–Parkin feedback amplification cycle and thereby foster the selective removal of protein aggregates from within mitochondria.

Results

Selective ΔOTC clearance via autophagy

Expression of a deletion mutant of mitochondrial ΔOTC produces an insoluble protein that localizes to the mitochondrial matrix and activates both the mitochondrial unfolded protein response (Zhao et al., 2002) and PINK1–Parkin-mediated mitophagy (Jin and Youle, 2013). To measure the relative contributions of PINK1 and Parkin to the removal of ΔOTC from cells, we took advantage of the fact the HeLa cells do not express endogenous Parkin (Denison et al., 2003). We confirmed by nested primer PCR and 5′ rapid amplification of cDNA ends (RACE) that HeLa cells lack Parkin expression (Fig. S1 A). We quantified WT OTC or ΔOTC degradation by inducing their expression with doxycycline (DOX; Fig. S1 B) followed by a 24 or 48 h washout of DOX in the presence or absence of PINK1 or Parkin. Western blot analysis revealed that ΔOTC expression decreased more rapidly than WT OTC in the presence of Parkin (Fig. 1, A and B; and Fig. S1 C). We confirmed that Parkin selectively enhanced ΔOTC removal by immunofluorescence (Fig. S1 D). Interestingly, when expressed in the same cell, WT OTC was not removed from mitochondria during Parkin-mediated elimination of ΔOTC after 24 or 48 h of DOX washout ($P < 0.01$; two-way ANOVA for the rate of WT OTC vs. ΔOTC removal after 48 h washout; Figs. 1 I and 8 D). ΔOTC removal was blocked in two independent CRISPR-generated PINK1 KO clones (Fig. 1, C and D; and Fig. S2, A and E) and rescued with infection of V5-His–tagged PINK1 in a PINK1 KO line (Fig. 1, C and D). Replication of cells did not dilute the ΔOTC signal appreciably as nocodazole treatment after DOX washout did not affect the clearance of ΔOTC (Fig. S2 B). Inhibition of autophagy by ATG5 KO (Fig. 1, E and F) and inhibition of lysosomal function by bafilomycin (Figs. 1 I and S2 B) blocked ΔOTC elimination even after 48 h of washout. Interestingly, in HeLa cells lacking Parkin, the levels of ΔOTC significantly decreased by 48 h of DOX washout and were dependent on lysosomal function (Fig. 1, A, B, G, and H). This Parkin-independent ΔOTC clearance was significantly blocked in PINK1 KO cells and rescued by viral infection with PINK1-V5 (Fig. 1, G and H). Therefore, ΔOTC can be cleared via the lysosome by PINK1 in the absence of Parkin, consistent with a prior study describing how PINK1 in the absence of Parkin is capable of recruiting autophagy adapters and inducing modest mitophagy (Lazarou et al., 2015). However, when expressed in the same cell, the difference in the removal rate between WT and ΔOTC in the absence of Parkin did not reach significance (Fig. S2 C). Therefore, the selectivity between misfolded and folded OTC is most clearly seen after local mitophagy amplification by Parkin.

Misfolded proteins can form focal inclusions in the mitochondrial matrix

To explore how PINK1 and Parkin mediate elimination of ΔOTC, we visualized WT OTC and ΔOTC localization by immunostaining cells inducibly expressing OTC at levels above the detection threshold of endogenous OTC (Fig. S2 D). Whereas WT OTC uniformly fills the mitochondrial matrix, ΔOTC forms focal aggregates in the mitochondrial matrix (Fig. 2, A and B). Parkin is recruited to ΔOTC containing mitochondria that maintain membrane potential (Jin and Youle, 2013). Parkin foci accumulated on intact polarized mitochondria and colocalized with or were directly adjacent to ΔOTC foci 67.5% of the time (Fig. 2, B–D). This focal localization of Parkin is reminiscent of bit-by-bit induction of mitophagy by Parkin (Yang and Yang, 2013) as well as mitophagy induced by the iron chelator deferiprone (Yamashita et al., 2016) and contrasts with the wholesale coating of mitochondria observed after treatment of cells with compounds or genetic stresses that depolarize mitochondria (Fig. S2 E; Narendra et al., 2008). We also treated cells with actinonin, which stalls mitochondrial translation and induces mitochondrial protein misfolding (Richter et al., 2013). Treatment of HeLa cells with actinonin caused YFP-Parkin to accumulate in focal spots on polarized mitochondrial subdomains (Fig. 2 E). Parkin was not recruited to mitochondria in PINK1 KO cells expressing ΔOTC (Fig. 2, F and G) or treated with actinonin (Figs. 2 H and S4 A). Parkin foci formation correlated with the fluorescence intensity of ΔOTC but not with mito-RFP intensity (Fig. S2 F), supporting the model that ΔOTC aggregate formation promotes stabilization of PINK1 and Parkin recruitment locally at sites of misfolded protein accumulation in the matrix. Immunostaining showed that more Parkin foci were found in ATG5 KO cells than in WT cells after DOX treatment (Fig. S3, A and B) and that small fragmented mitochondria coated in Parkin accumulated after a 16-h treatment with actinonin in ATG5 KO cells or after a 24-h washout of DOX in cells treated with bafilomycin (Fig. S3, C and D). We previously showed that overexpressed PINK1-YFP coats the entire mitochondrial network after 72 h of ΔOTC induction (Jin and Youle, 2013), unlike the focal Parkin spots seen after 48 h DOX treatment. Therefore, we determined whether this was caused by excessive transient overexpression by developing a stably transfected HeLa cell line with lower levels of PINK1. We validated the specificity of PINK1 labeling also by assessing the lack of labeling in PINK1 KO cells and in cells not treated with DOX (Fig. 2 I). After 72 h of ΔOTC induction, PINK1 was found in focal spots on mitochondria specifically in cells expressing ΔOTC (Fig. 2 I), consistent with the essential role of PINK1 in recruiting Parkin to focal sites on mitochondria (Fig. 2, F–H; and Fig. S4 A).

Autophagy receptors and LC3 are recruited to Parkin foci in ΔOTC-expressing cells

Ubiquitin accumulated and colocalized with Parkin and ΔOTC aggregates on mitochondria but not in cells expressing WT OTC (Fig. 3 A), consistent with activation of Parkin E3 ubiquitin ligase activity by PINK1 (Pickrell and Youle, 2015). Confocal and superresolution imaging revealed that optineurin, an autophagy receptor that is recruited to mitochondria after Parkin activation (Wong and Holzbaur, 2014; Heo et al., 2015; Lazarou et al., 2015), is recruited to subdomains of intact mitochondria (Fig. 3 C) that colocalize with both Parkin and ΔOTC (Fig. 3, B and C; and Fig. S4 B). LC3 can also colocalize with Parkin foci in ΔOTC-expressing cells (Figs. 3 D and S4 B). Live-cell imaging confirmed that

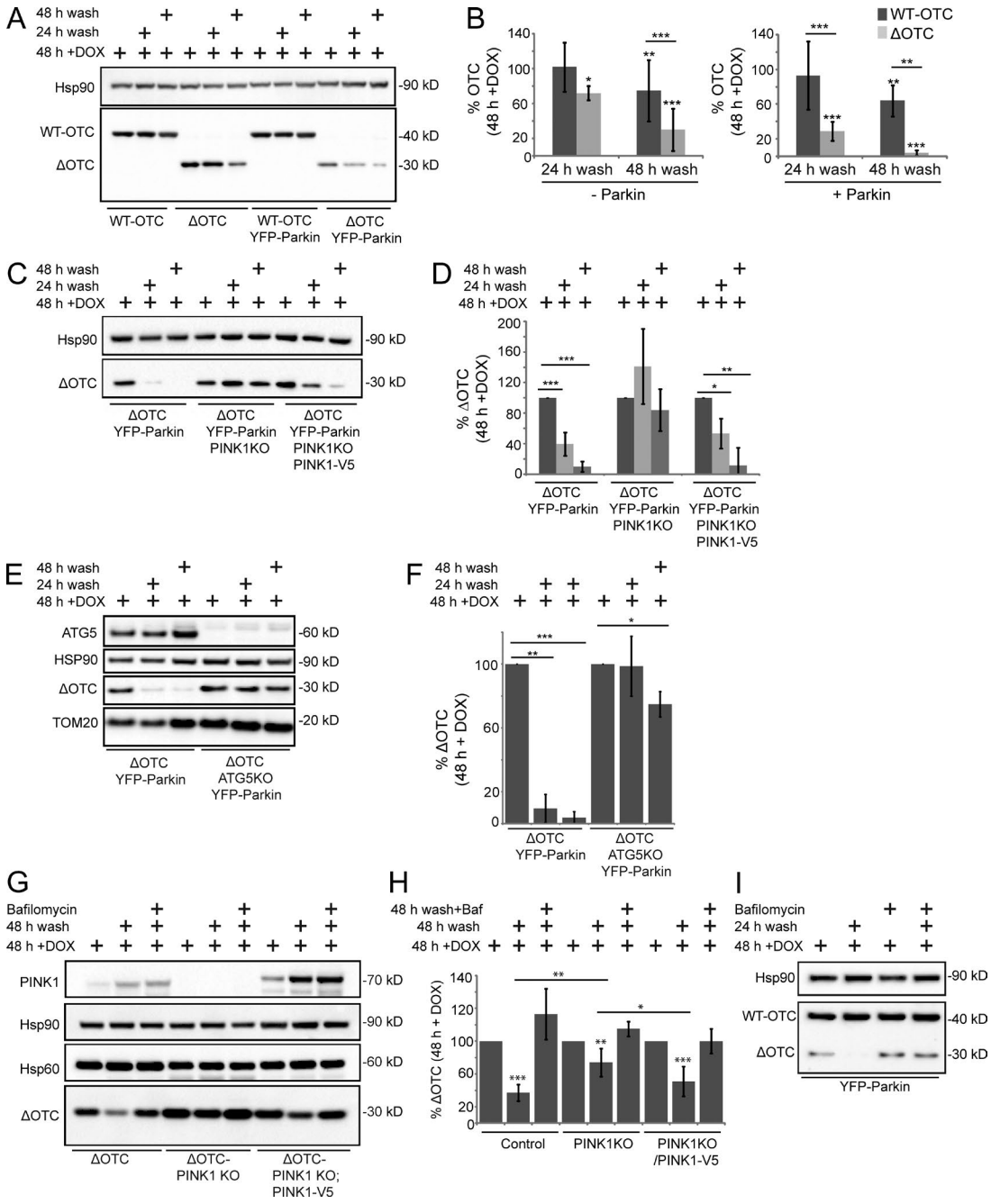

Figure 1. **PINK1–Parkin regulate misfolded protein clearance from mitochondria.** (A) Tet ON: WT OTC or ΔOTC-expressing HeLa cells with or without YFP-Parkin expression were treated with DOX for 48 h or for 48 h with a 24- or 48-h washout of DOX and then processed for Western blot analysis. (B) Quantification of Western blots described in A expressed as the percentage of OTC levels relative to OTC levels after 48 h DOX treatment normalized to Hsp90 levels. $n \geq 4$. For left graphs, from left to right, *, P = 0.03; **, P = 0.008; ***, P = 0.0004; ***, P = 0.0001; for right graphs, ***, P = 5.8×10^{-5}; ***, P = 0.0001; **, P = 0.007; **, P = 0.0011; ***, P = 6.7×10^{-9}. Asterisks lacking a black underline represent significance values relative to OTC levels after 48 h DOX treatment (i.e., 100%). (C) Western blot of Tet ON: ΔOTC-expressing HeLa cells with YFP-Parkin expression with or without a PINK1 KO background and with or without PINK1-V5 expression were treated with DOX for 48 h or for 48 h with a 24 or 48 h washout of DOX. (D) Quantification of Western blots described in C and expressed as the percentage of ΔOTC levels relative to ΔOTC levels after 48 h DOX treatment normalized to Hsp90 levels. $n \geq 4$. From left to right, ***, P = 2.4×10^{-6}; ***, P = 3×10^{-8}; *, P = 0.045; **, P = 0.006. (E) Western blot of Tet-ON: ΔOTC-expressing HeLa cells expressing YFP-Parkin with or without an ATG5 KO background treated with DOX for 48 h or with DOX for 48 h followed by a 24- or 48-h washout of DOX. (F) Quantification of Western blots described in E expressed as the percentage of ΔOTC levels relative to ΔOTC levels after 48 h DOX treatment normalized to Hsp90 levels. $n = 3$. From left to right, **, P = 0.003; ***, P = 0.0005; *, P = 0.03. (G) Tet-ON: ΔOTC-expressing HeLa cells without Parkin expression, with or without a PINK1 KO background, and with or without PINK1-V5 expression were treated with DOX for 48 h or for 48 h with a 48-h washout of DOX and with or without 100 nM bafilomycin and 20 μM QVD treatment and then processed for Western blot analysis. (H) Quantification of Western blots as described in G expressed as the percentage of ΔOTC levels relative to ΔOTC levels after 48 h DOX treatment normalized to Hsp90 levels. $n \geq 3$. From left to right, ***, P = 9.93×10^{-5}; **, P = 0.002; **, P = 0.008; *, P = 0.036; ***, P = 0.0005. (I) Western blot of HeLa cells stably expressing Tet-ON: WT OTC and ΔOTC in the same cell with YFP-Parkin expression after treatment with DOX for 48 h or 48 h with a 24-h washout of DOX with or without 200 nM bafilomycin treatment and 20 μM QVD after washout. Error bars indicate SD.

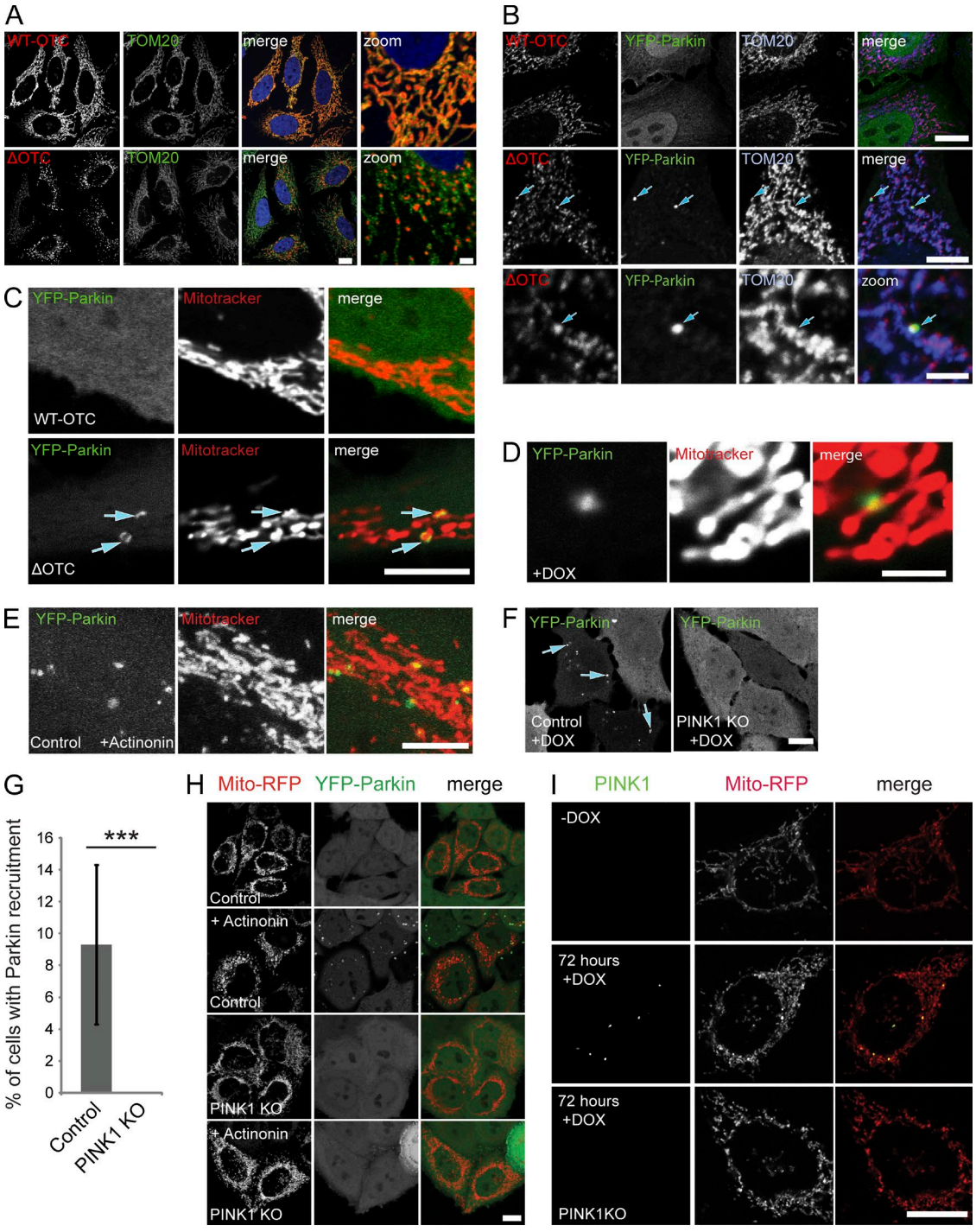

Figure 2. **Parkin is recruited by PINK1 to focal sites on mitochondria that harbor matrix-localized misfolded protein aggregates.** (A) Tet-ON: WT OTC or ΔOTC-expressing HeLa cells were treated with DOX for 48 h and then fixed and stained with antibodies against OTC (red) and Tom20 (green). Bars: (left) 10 µm; (right) 2 µm. (B) Tet-ON: WT OTC or ΔOTC-expressing HeLa cells expressing YFP-Parkin (green) were treated with DOX for 48 h and then fixed and stained for OTC (red) and TOM20 (blue). The blue arrows indicate YFP-Parkin foci that colocalized with ΔOTC. Bars: (top and middle) 10 µm; (bottom) 5 µm. (C) Tet-ON: WT OTC or ΔOTC-expressing cells expressing YFP-Parkin (green) were treated with DOX for 48 h, labeled with MitoTracker deep red (red), and imaged live. Blue arrows indicate YFP-Parkin foci that localized on polarized mitochondria. Bar, 5 µm. (D) Tet-ON: ΔOTC-expressing cells expressing YFP-Parkin (green) were treated with DOX for 48 h, labeled with MitoTracker deep red (red), and imaged live. Bar, 2 µm. (E) HeLa cells expressing YFP-Parkin (green) were treated with actinonin for 4 h, labeled with MitoTracker CMXRos (red), and imaged live. Bar, 5 µm. (F) Tet-ON: ΔOTC-expressing HeLa cells expressing YFP-Parkin with or without a PINK1 KO background were treated with DOX for 48 h, fixed, and imaged. Blue arrows indicate YFP-Parkin foci that localized on mitochondrial subdomains. Bar, 10 µm. (G) Quantification of the percentage of cells with Parkin recruitment in Tet-ON: ΔOTC-expressing HeLa cells with or without a PINK1 KO background after treatment with DOX for 48 h. $n = 3$; $N \geq 400$. ***, $P < 0.001$. The error bar indicates SD. (H) HeLa cells stably expressing YFP-Parkin with or without a PINK1 KO background expressing mito-RFP (red) were treated with vehicle (DMSO) or 150 µM actinonin for 6 h, fixed, and imaged. Bar, 10 µm. (I) PINK1 KO Tet ON: ΔOTC-expressing HeLa cells expressing PINK1-V5-His (green) and mito-RFP (red) with and without DOX treatment for 72 h were processed for immunostaining. Uninfected PINK1 KO cells were stained as a negative control. Bar, 10 µm.

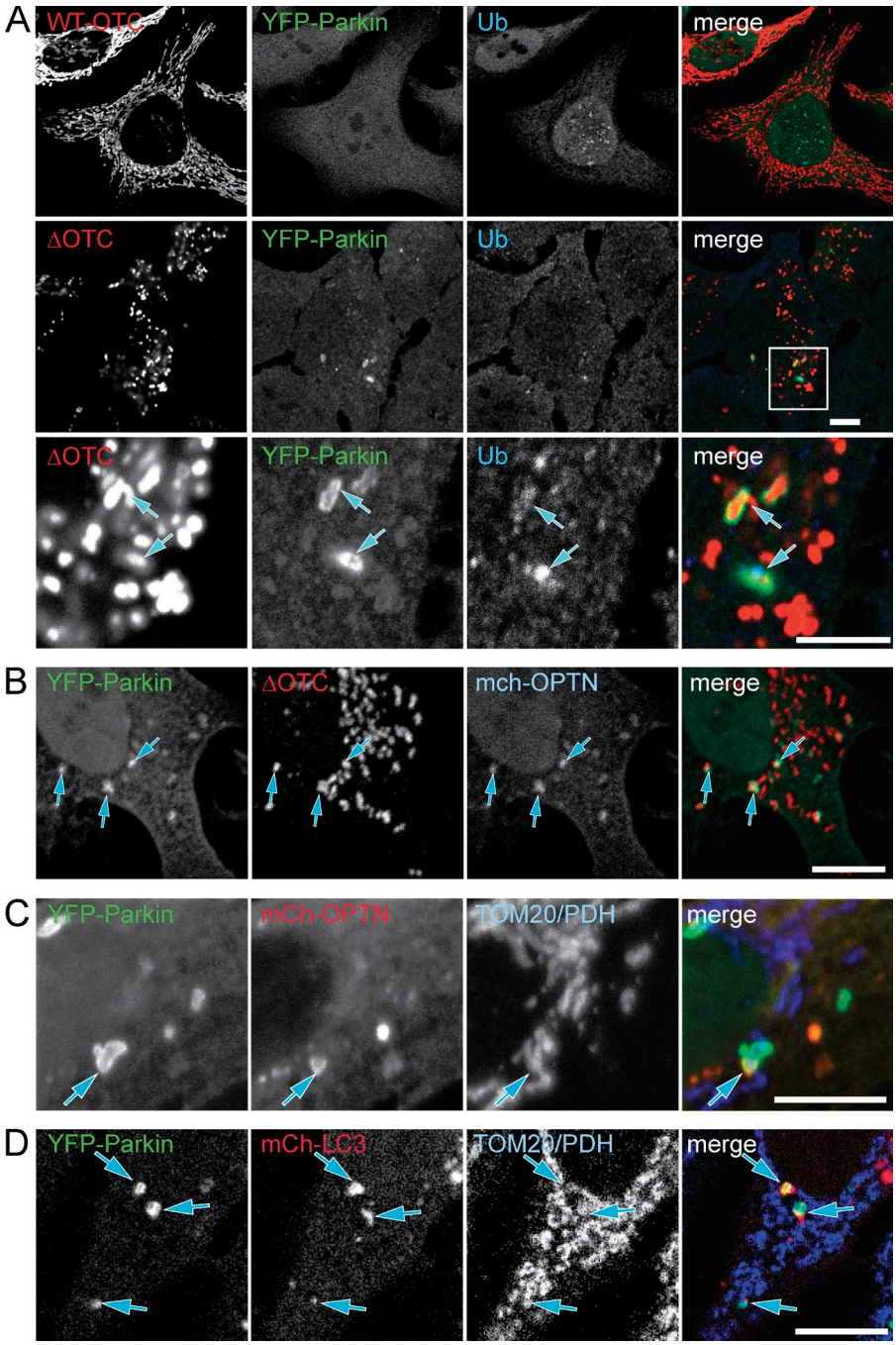

Figure 3. **Autophagy machinery is recruited at focal sites on mitochondria containing misfolded protein aggregates.** (A) Tet-ON: WT OTC or ΔOTC-expressing cells expressing YFP-Parkin (green) were treated with DOX for 48 h and processed for indirect immunofluorescence microscopy with antibodies against OTC (red) and ubiquitin (Ub; blue). (B) Tet ON: ΔOTC-expressing HeLa cells expressing YFP-Parkin (green) and mCherry-optineurin (mCh-OPTN; blue) were fixed and stained with an antibody against OTC (red). (C) Tet ON: ΔOTC-expressing HeLa cells expressing YFP-Parkin (green) and mCherry-optineurin (red) were fixed and stained with antibodies against TOM20 and PDH (blue). A super-resolution Airyscan is depicted. (D) Tet ON: ΔOTC-expressing HeLa cells also expressing YFP-Parkin (green) and mCherry-LC3 (red) were fixed and stained with antibodies to TOM20 and PDH (blue). For A–D, blue arrows denote Parkin foci that colocalized with ΔOTC, optineurin, ubiquitin, or LC3 on mitochondria, respectively. Bars: (A, top, and B–D) 10 µm; (A, bottom) 5 µm.

LC3 is recruited to Parkin-positive foci, which can detach from the intact mitochondrial network (Video 1). After 48 h of ΔOTC induction, optineurin and LC3 were occasionally localized with ΔOTC in cells lacking Parkin expression but at a lower frequency than in cells expressing Parkin (Fig. 4, B–D), whereas ubiquitin associated with ΔOTC was generally below the level of detection in the absence of Parkin, likely reflecting the lack of ubiquitination by Parkin (Fig. 4, B–D). PINK1 KO dramatically diminished the frequency of optineurin and LC3 localization with mitochondria in cells with or without Parkin expression (Fig. 4 A). These results support the model that PINK1 recruits Parkin to sites of local damage on mitochondria and causes local assembly of the autophagy machinery.

Parkin forms foci on polarized mitochondrial subdomains before Drp1-mediated fission

Mitochondrial fission has been shown to partition mitochondrial fragments that have an increased probability of being degraded via autophagy (Twig et al., 2008; Yang and Yang, 2013). Therefore, we assessed the role of fission and Drp1 in misfolded protein elimination. After a 48-h induction, and more pronounced after a 72-h induction, mitochondria fragmented in cells expressing ΔOTC but not in those expressing WT OTC (Fig. 5, A and B). The presence of Parkin foci in cells correlated with mitochondrial fragmentation (Fig. 5, A, C, and D), and the frequency of cells with fragmented mitochondria decreased significantly in cells lacking PINK1 expression (Fig. 5, C and D).

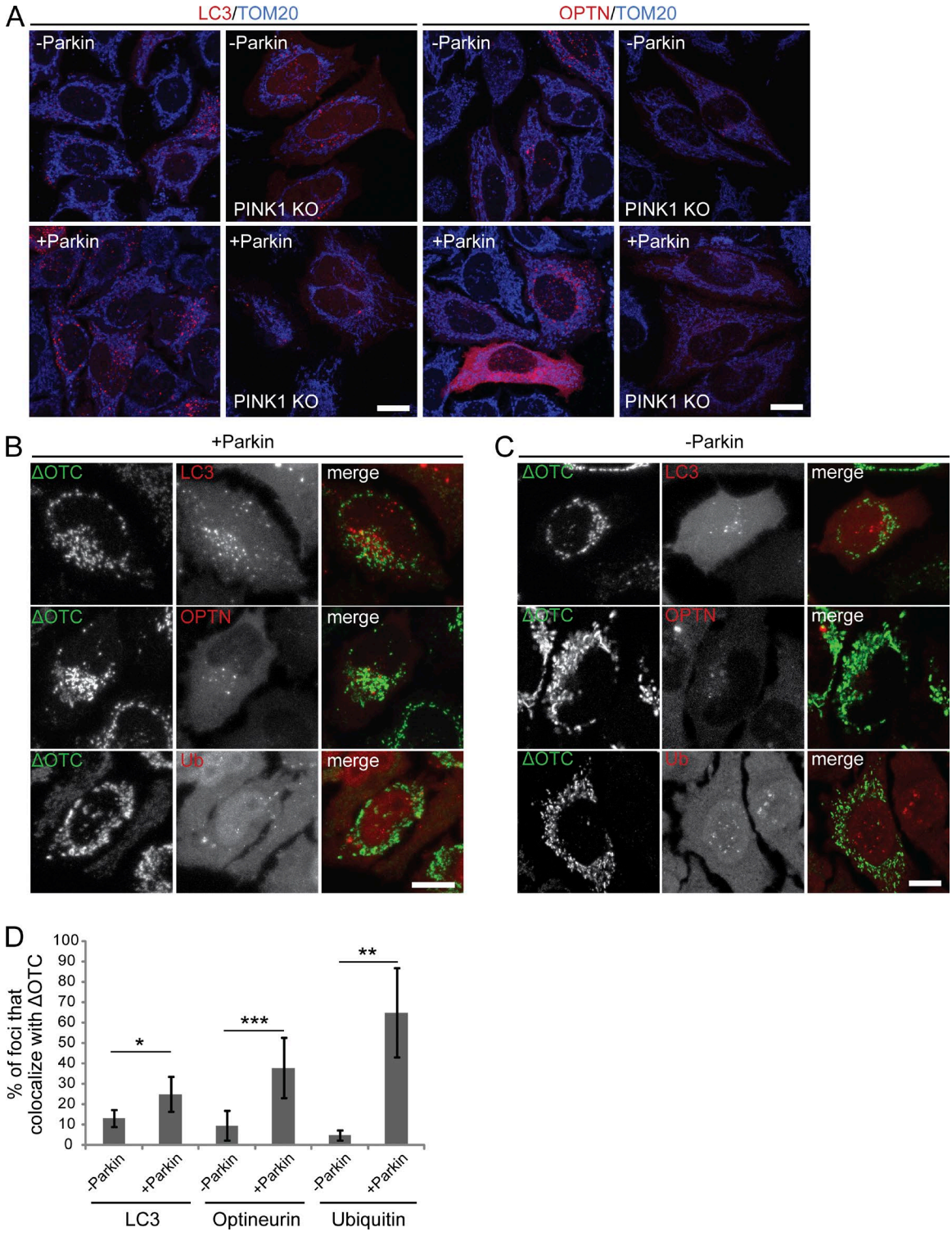

Figure 4. **Autophagy factors colocalize with ΔOTC foci in a PINK1-dependent manner.** (A) Tet ON: ΔOTC-expressing HeLa cells with or without a PINK1 KO background and with or without YFP-Parkin expression expressing mCherry-LC3 (LC3; red) or mCherry-optineurin (OPTN; red) were treated with DOX for 48 h, fixed, stained for TOM20 (blue), and imaged. (B) Tet-ON: ΔOTC-expressing cells with YFP-Parkin expression with or without mCherry-LC3 or mCherry-optineurin (red) expression were treated with DOX for 48 h and processed for indirect immunofluorescence microscopy with an antibody against OTC (green) and ubiquitin (Ub; red).Bar, 10 µm. (C) Tet-ON: ΔOTC-expressing cells without YFP-Parkin expression with or without mCherry-LC3 or mCherry-optineurin (red) expression were treated with DOX for 48 h and processed for indirect immunofluorescence microscopy with an antibody against OTC (green) and ubiquitin (red). Bars, 10 µm. (D) Quantification of the percentage of foci of LC3, optineurin, or ubiquitin that colocalize with ΔOTC in the cells with and without Parkin expression as described in B and C. *, $P < 0.05$; **, $P < 0.01$; ***, $P < 0.001$. Error bars indicate SD.

In ΔOTC-expressing cells or cells treated with actinonin, mitochondrial subdomains associated with Parkin were observed to fragment and traffic away from their parental mitochondrion (Fig. 6 A and Videos 1, 2, 3, and 4). To examine the dynamics of mitochondrial subdomains, we fused ΔOTC to a SNAP tag (Keppler et al., 2002) for use in live-cell imaging. Fractionation and Western blot analysis of ΔOTC-SNAP revealed that ΔOTC-SNAP was mainly present in the detergent-insoluble fraction (Fig. S4 E) as has been previously demonstrated for untagged ΔOTC (Zhao et al., 2002; Jin and Youle, 2013). Parkin foci were found associated with mitochondrial subdomains containing ΔOTC-SNAP that could break away from their parental mitochondrion and retain the misfolded protein aggregate inside the Parkin-coated fission product (Fig. S4 C). Long-term imaging revealed that after asymmetric fission, Parkin remained coating fragmented mitochondrial subdomains containing ΔOTC-SNAP (Fig. S4 D). To determine whether fission of mitochondrial subdomains required Drp1, we live imaged control cells and cells expressing a dominant negative mutant of Drp1, Drp1K38A (Smirnova et al., 2001), or Drp1 KO cells. After ΔOTC induction, cells lacking Drp1 or expressing Drp1 K38A displayed significantly less fission and trafficking of Parkin-coated mitochondrial subdomains than control cells (Fig. 6, B and C; and Video 5), indicating that they represent mitochondrial fragments and not mitochondrial-derived vesicles (MDVs; Soubannier et al., 2012).

Drp1 is not required for clearance of protein aggregates

Although Drp1 has been reported to be required for mammalian mitophagy, there is mixed evidence on this issue (Graef, 2016). To assess whether mitochondrial fission is required for ΔOTC clearance, we overexpressed a dominant-negative mutant of Drp1 in the ΔOTC-inducible cell line and found that Drp1K38A expression did not inhibit ΔOTC clearance (Fig. S4 F). We also knocked out Drp1 in the ΔOTC-inducible cell line using CRISPR-mediated gene editing. In contrast to the loss of ATG5 (Fig. 1, E and F), knocking out Drp1 had no effect on the rate of ΔOTC removal (Fig. 6, D and E; and Fig. S4 G). Bafilomycin inhibited the loss of ΔOTC regardless of the presence of Drp1 (Fig. 6, D and E). Thus, paradoxically, loss of Drp1 inhibits fission of mitochondrial subdomains harboring ΔOTC but not mitophagy of the protein aggregates within these subdomains. Live imaging of YFP-Parkin–expressing cells transfected with mCherry-Drp1 after treatment with actinonin for 4–6 h and labeling of these cells with MitoTracker deep red revealed that Drp1 could be recruited to Parkin foci on mitochondrial subdomains (Fig. S4 H). After Drp1 recruitment, Parkin-coated mitochondrial subdomains could break off and traffic away from the parental mitochondrion (Fig. S4 H and Videos 6 and 7). Quantification of the percentage of cells with Parkin recruitment showed that in both control and Drp1 KO lines, the fraction of cells that displayed Parkin recruitment after washout of DOX was consistent with the timing of ΔOTC clearance seen by Western blotting (Figs. 1 A and 7, A and C). By hour 48 of washout of DOX, both control and Drp1 KO cells displayed a significant decrease in the percentage of cells with Parkin recruitment (Fig. 7, A and C). Endogenous Drp1 foci were frequently localized to mitochondria with or without Parkin expression and did not detectably increase upon proteotoxic stress (Figs. 7 B and S5, E and F). However, 74.6% of Parkin foci on mitochondria after DOX treatment colocalized with Drp1, supporting the model that Drp1 facilitates selective removal of misfolded proteins by mediating fission.

Selectivity of the PINK1–Parkin pathway is lost after Drp1 inhibition

To explore how ΔOTC is degraded in the absence of Drp1, we imaged WT OTC and ΔOTC-expressing cells also expressing Drp1K38A. As in control cells (Fig. 2 A), WT OTC is distributed evenly throughout the elongated mitochondrial matrix, whereas ΔOTC is in focal aggregates (Fig. 8 A). Unexpectedly, inhibiting mitochondrial fission with Drp1K38A enhanced Parkin translocation in ΔOTC-expressing cells and induced Parkin recruitment even in cells expressing WT OTC (Figs. 8 B and S5 A), which was not observed in the absence of Drp1K38A. Similarly, Parkin accumulated on mitochondria in 13.1 ± 11% of Drp1 KO cells without induction of ΔOTC (Figs. 8 C and S5 B), a phenomenon not seen in WT cells. In contrast to the focal recruitment of Parkin observed in WT cells expressing ΔOTC, Parkin often coated long segments of the fused mitochondrial network in cells lacking Drp1 function (Fig. 8 C). We also knocked out Drp1 in WT HCT116 cells and in WT HeLa cells expressing YFP-Parkin. Constitutive Parkin recruitment to mitochondria occurred in both of these Drp1 KO cell lines grown under steady-state conditions (Figs. 8 F and S5 B). After induction of ΔOTC in Drp1 KO cells, ∼20% of cells displayed Parkin recruitment (Fig. S5 B). Within this population, 52% of cells were found to display wholesale coating of large segments of the mitochondrial network, with the remainder displaying focal Parkin recruitment. Interestingly, Parkin-coated areas of the mitochondrial membrane that lacked membrane potential and areas that maintained membrane potential as detected by tetramethylrhodamine, methyl ester (TMRM) staining (Fig. 8 C, middle). Parkin accumulation in both areas was blocked by knockdown of PINK1 (Fig. S5 C). These results suggest that loss of mitochondrial fission impairs mitochondrial function and that damage accumulates to an extent that activates the PINK1–Parkin pathway even in the absence of mitochondrial depolarization. Furthermore, the loss of Drp1 appears to foster excessive PINK1–Parkin-mediated mitophagy of entire fused mitochondrial networks. To test this model, we knocked out Drp1 in cells capable of inducibly expressing both WT OTC and ΔOTC in the same cell. In contrast to control HeLa cells (Figs. 1 I and 8 D), in Drp1 KO cells, both ΔOTC and WT OTC were cleared at similar rates (Fig. 8, D and E). Endogenous mitochondrial Hsp60 levels remained unchanged at all time points, suggesting that ongoing translation of mitochondrial proteins masked the mitophagy. To corroborate the increase in mitophagy in the absence of Drp1, we transiently infected mitochondrial-targeted GFP to yield a transient bolus of mitochondrial protein to compare with the pulse chase method of DOX-induced OTC expression. Like ΔOTC, mito-GFP expression decreased faster in Drp1 KO cells, and the decrease was inhibited by bafilomycin (Figs. 8 G and S5, G and H). These results suggest that loss of Drp1 impairs selective clearance of mitochondrial subdomains, leading to the spread of Parkin activation along the mitochondrial surface and mitophagy that consumes even WT OTC. We used the sensitive, quantitative, and observer-independent mito-Keima FACS assay to compare mitophagy in the presence and absence of Drp1 (Katayama et al., 2011; Lazarou et al., 2015). Under steady-state growth, Drp1 KO cells show a substantial increase in the fraction of cells undergoing mitophagy relative to WT

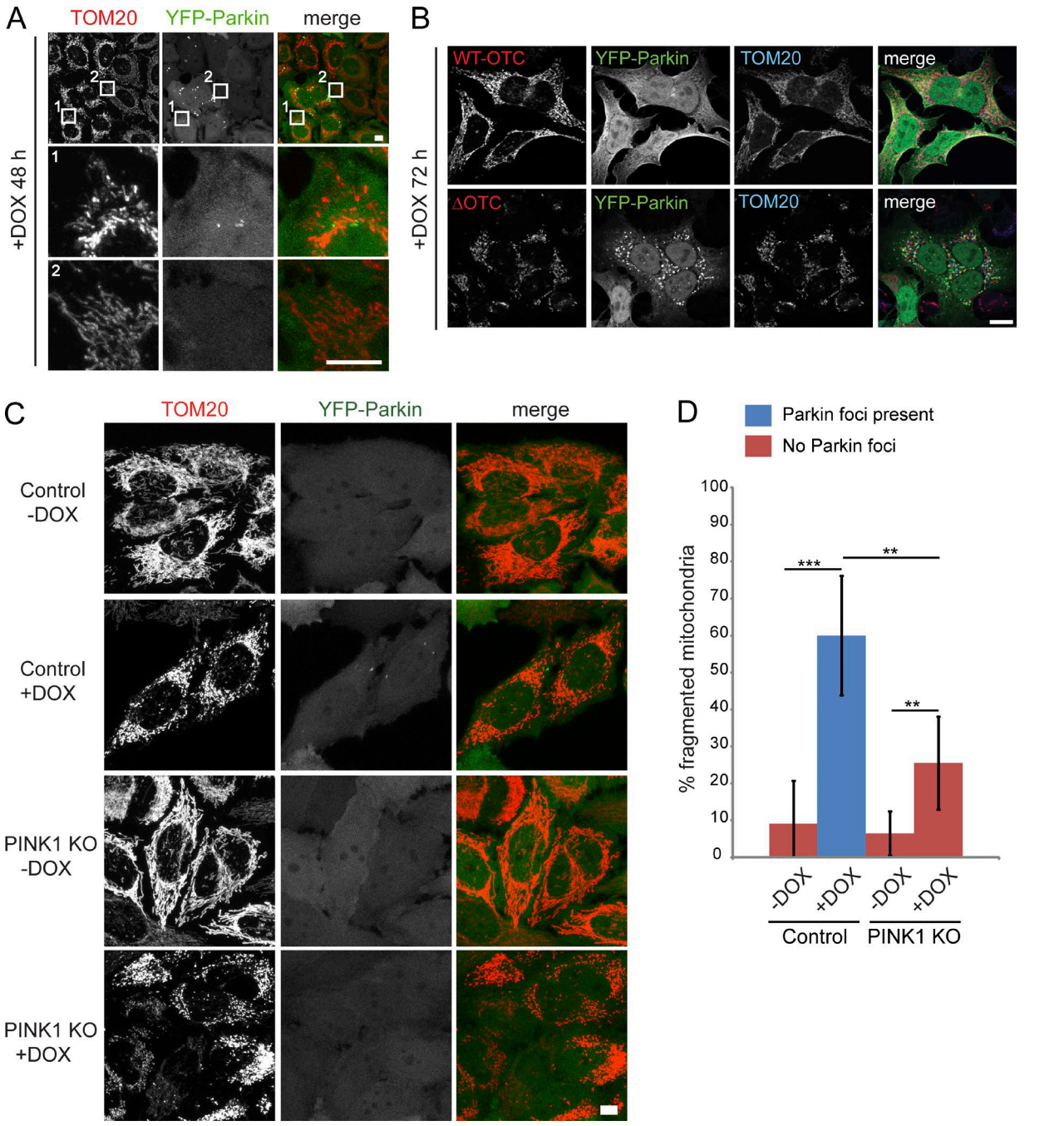

Figure 5. **Proteotoxic stress induces mitochondrial fission in a PINK1-dependent manner.** (A) Tet ON: ΔOTC-expressing HeLa cells expressing YFP-Parkin (green) were treated with DOX for 48 h, stained for TOM20 (red), and imaged. Boxes mark cropped images shown below. (B) Tet ON: WT OTC or ΔOTC-expressing HeLa cells expressing YFP-Parkin (green) were treated with DOX for 72 h, stained for OTC (red) and TOM20 (blue), and imaged. (C) Tet ON: ΔOTC-expressing HeLa cells expressing YFP-Parkin (green) with or without treatment with DOX for 48 h and with or without a PINK1 KO background were stained for TOM20 (red) and imaged. Bars: (A, top, and B and C) 10 µm; (A, bottom) 5 µm. (D) Quantification of the percentage of cells with fragmented mitochondria that also do or do not display focal Parkin recruitment in the cells described in C. **, $P < 0.01$; ***, $P < 0.001$. Error bars indicate SD.

cells (Figs. 9 A and S5 D). Loss of Drp1 also amplified the level of mitophagy severalfold when inducing mitophagy with the mitochondrial uncoupler oligomycin/antimycin A (OA) or with ΔOTC (Fig. 9, A and B; and Fig. S5 D). These results support the conclusion that Drp1 is not required for mitophagy in mammalian cells, consistent with a recent study (Yamashita et al., 2016), and that Drp1 KO enhances mitophagy flux.

Autophagy factors are recruited to mitochondria in Drp1 KO cells

In contrast with control cells that exhibit focal recruitment of ubiquitin, LC3, and optineurin (Fig. 3), after DOX induction of Drp1 KO cells, ubiquitin, optineurin and p62, but not LC3, often coat large segments of Parkin-positive mitochondrial networks (Fig. 9 C). In WT cells, actinonin caused ubiquitin and

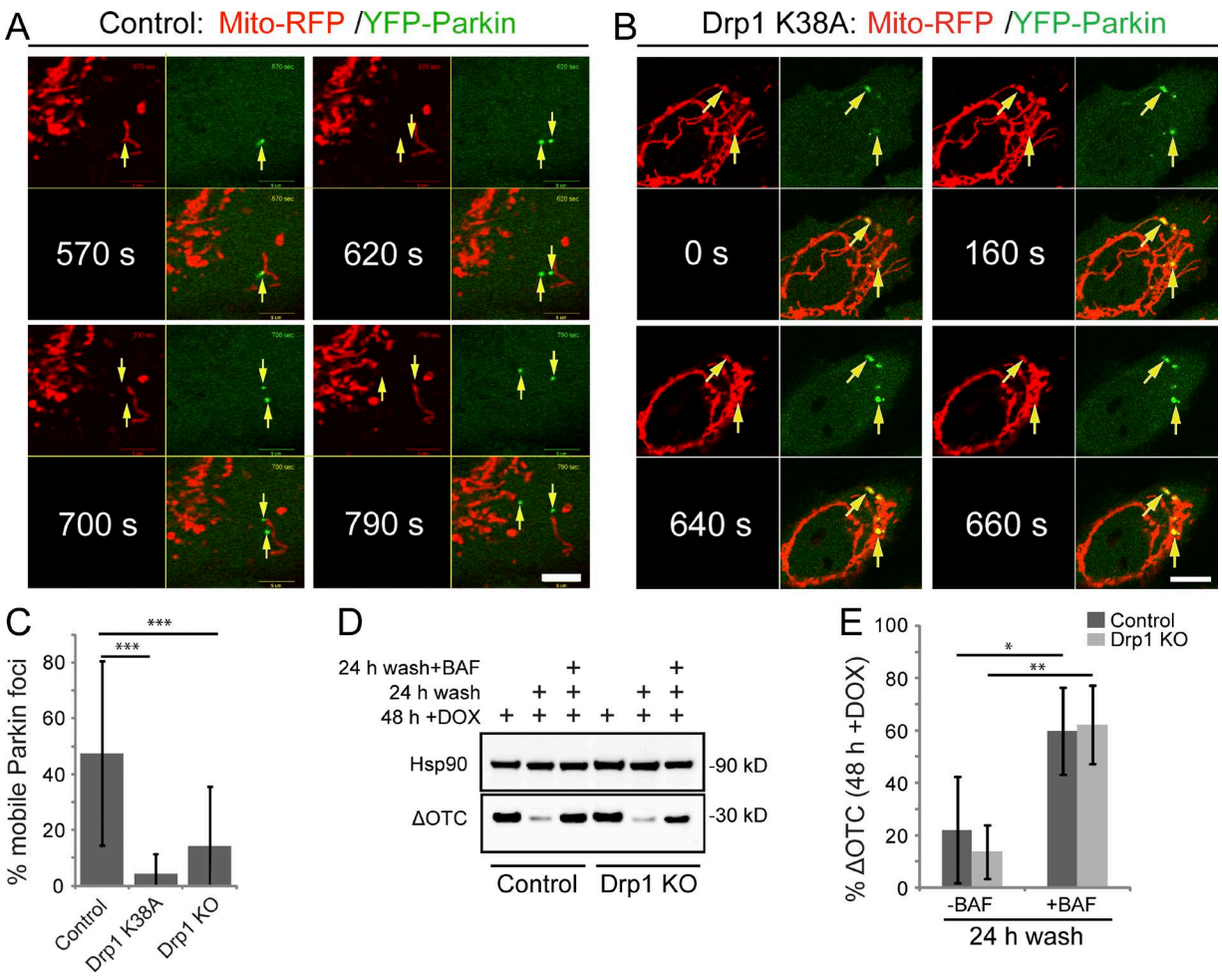

Figure 6. **Drp1 is required for fission of subdomains harboring ΔOTC but not ΔOTC clearance.** (A) Tet ON: ΔOTC-expressing HeLa cells expressing YFP-Parkin (green) and mito-RFP (red) were imaged live over the indicated time points. Yellow arrows mark a Parkin focus that fragmented and trafficked away from a mitochondrion. (B) Tet-ON: ΔOTC-expressing HeLa cells expressing YFP-Parkin (green), mito-RFP (red), and Drp1K38A were imaged live over the indicated time points. Yellow arrows denote the location of immobile Parkin foci on the intact mitochondrial network. Bars, 10 µm. (C) Quantification of the percentage of cells with mobile Parkin foci that underwent fission events from mitochondrial subdomains in Tet-ON: ΔOTC-expressing HeLa cells expressing YFP-Parkin with or without Drp1 inhibition after 48 h DOX treatment. For control and Drp1 KO, $n \geq 3$; $n \geq 20$. For Drp1 K38A, $n = 2$; $n \geq 10$. (D) Tet-ON: ΔOTC-expressing HeLa cells with or without a Drp1 KO background expressing YFP-Parkin were treated with DOX for 48 h or 48 h with a 24-h washout of DOX with or without treatment with 200 nM bafilomycin and 20 µM QVD and then processed for Western blot analysis. (E) Quantification of Western blots as described in D and expressed as the percentage of ΔOTC levels after 48 h DOX treatment after normalization to Hsp90 levels. $n = 4$. *, $P < 0.05$; **, $P < 0.01$; ***, $P < 0.001$. Error bars indicate SD.

p62 recruitment to focal spots on mitochondria that colocalized with Parkin (Fig. 9, D and E). However, in Drp1 KO cells, actinonin treatment caused robust wholesale coating of the mitochondrial network by Parkin, ubiquitin, and p62 (Fig. 9, D and E). Treatment with actinonin for 4–6 h caused mitochondrial fragmentation in control cells but not in Drp1 KO cells (Fig. 9, D and E). However, long-term exposure to actinonin (>6 h) or ΔOTC caused Drp1-independent fission and fragmentation of Parkin-coated mitochondrial networks (Fig. 9 F and Videos 8 and 9) that may be mediated by dynamin 2 (Lee et al., 2016). Long-term live imaging of cells treated with actinonin revealed that Parkin foci remained relatively stable on intact mitochondria but could eventually fragment off the parental mitochondrion or occasionally spread to adjacent regions of the mitochondrial network (Video 8). We also observed mitochondrial membrane potential fluctuations in Drp1 KO cells as previously described (Roy et al., 2016). In Drp1 KO cells expressing ΔOTC and YFP-Parkin, we observed membrane potential fluctuations followed by enhanced recruitment of Parkin to elongated mitochondria (Video 10).

Syntaxin 17 KO does not affect actinonin-induced mitophagy in Drp1 KO cells

MDVs have numerous functions including the trafficking of damaged mitochondrial proteins to lysosomes for degradation. This subclass of MDVs requires PINK1–Parkin and syntaxin 17 but acts independently of Drp1 and autophagy (Soubannier et al., 2012; McLelland et al., 2016). Therefore, to assess whether Drp1-independent mitophagy involved MDVs, we knocked down syntaxin 17 and assayed ΔOTC clearance in either control or Drp1 KO cells (Fig. 10, A and B). Although the rate of ΔOTC clearance was enhanced in Drp1 KO cells and ΔOTC clearance was blocked by PINK1 knockdown in both control and Drp1 KO cells, syntaxin 17 siRNA did not inhibit ΔOTC clearance (Fig. 10, A and B). To corroborate this result, we created syntaxin 17/Drp1 double-KO cell lines (Fig. 10 C), treated

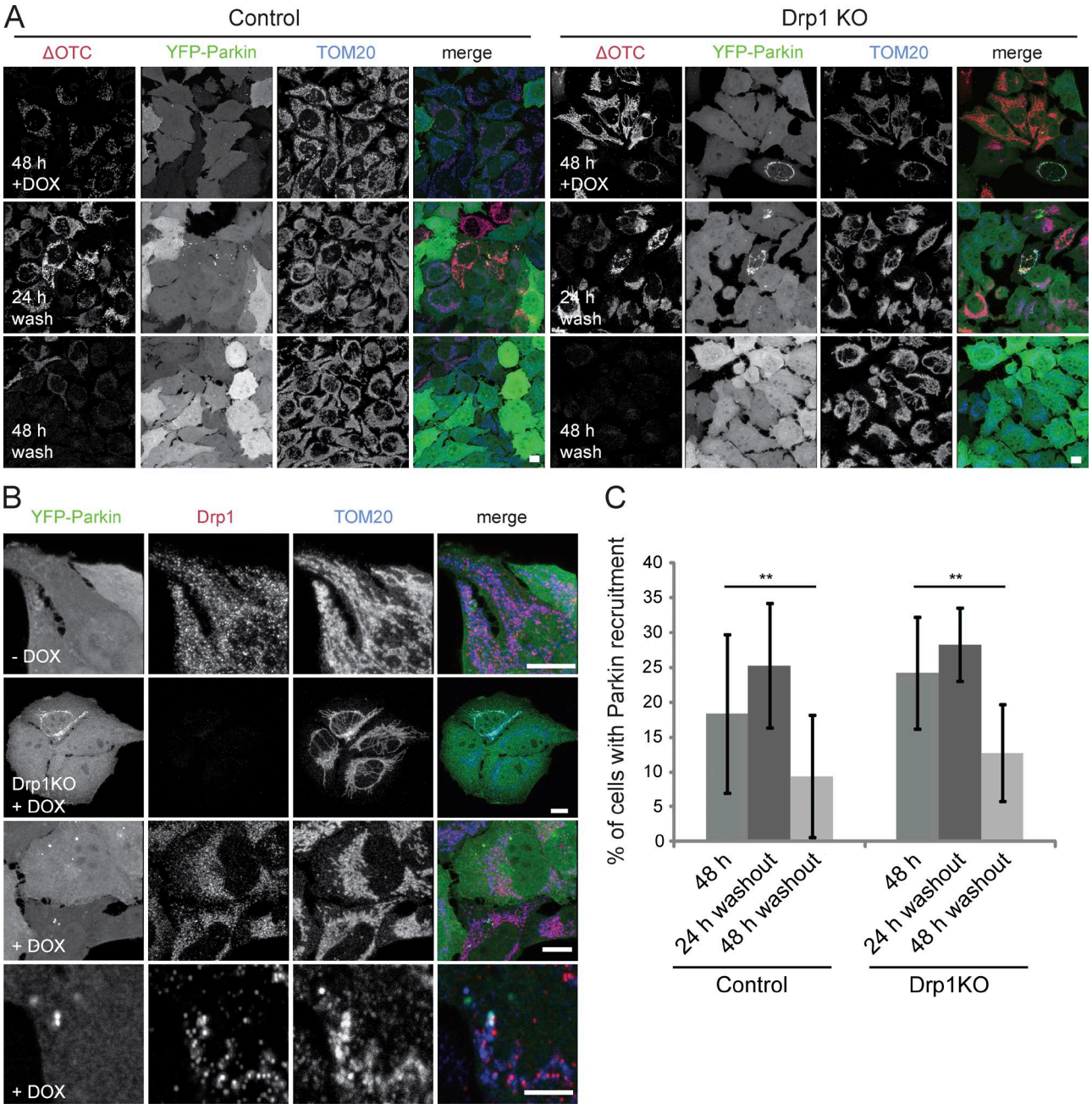

Figure 7. **Drp1 is recruited to Parkin foci and triggers fission of mitochondrial subdomains coated in Parkin.** (A) Tet-ON: ΔOTC-expressing HeLa cells expressing YFP-Parkin (green) with or without a Drp1 KO background were treated with DOX for 48 h or for 48 h with a 24- or 48-h washout of DOX. Cells were fixed and stained for TOM20 (blue) and ΔOTC (red). (B) Tet-ON: ΔOTC-expressing HeLa cells expressing YFP-Parkin (green) with or without a Drp1 KO background with or without DOX treatment were fixed for 48 h and stained for Drp1 (red) and TOM20 (blue). Bars: (A and B, top) 10 µm; (B, bottom) 5 µm. (C) Quantification of the percentage of cells described in A with Parkin foci recruitment to mitochondria. $n = 3$. **, $P < 0.01$. Error bars indicate SD.

these and Drp1 KO (control) cells with actinonin for 12–16 h, and analyzed mitochondrial Hsp60 and TIM23 levels by Western blot. Syntaxin 17 KO had no effect on actinonin-induced mitophagy in Drp1 KO cells (Fig. 10, D and E).

Discussion

Accumulation of misfolded proteins in mitochondria stemming from mitochondrial DNA (mtDNA) mutations, oxidative damage, or a misbalance between mitochondrial- and nuclear-encoded gene products has been proposed to underlie the etiology of numerous mitochondrial-associated diseases (Nunnari and Suomalainen, 2012). The mitochondrial-unfolded protein response and mitophagy are two pathways that may mitigate misfolded protein accumulation (Jin and Youle, 2013; Lin et al., 2016). In *Caenorhabditis elegans*, Drp1 and the mitochondrial unfolded protein response appear to compensate for a deleterious mtDNA mutation (Lin et al., 2016). Similarly, genetic manipulations in flies that promote fission rescue phenotypes associated with *PINK1* and *parkin* mutations and aging (Deng et al., 2008; Poole et al., 2008; Burman et al., 2012). Addition-

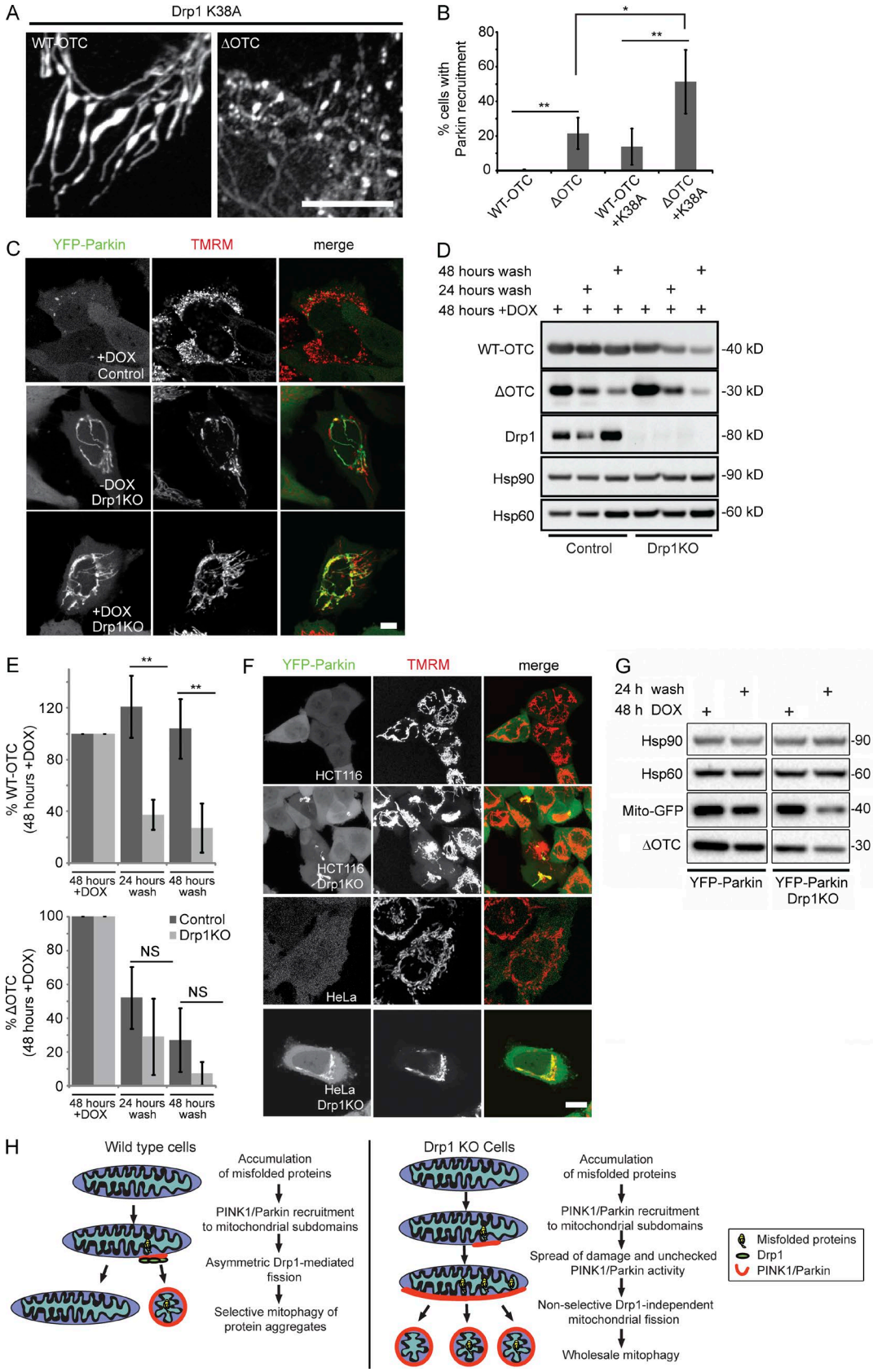

Figure 8. **Drp1 functions to prevent wholesale mitophagy by restricting PINK1–Parkin activity to mitochondrial subdomains.** (A) Tet ON: WT OTC or ΔOTC-expressing HeLa cells expressing Drp1 K38A were treated with DOX for 48 h and then processed for indirect immunofluorescence with an antibody to OTC. (B) Quantification of the percentage of cells with Parkin recruitment in control and Drp1 K38A expressing Tet ON: WT OTC or ΔOTC HeLa cells that also express YFP-Parkin. $n = 2$; $n \geq 50$. (C) Tet-ON: ΔOTC-expressing cells expressing YFP-Parkin (green) with or without a Drp1 KO background with

ally, endogenous Parkin was found to rescue dopaminergic neurons in vivo from mtDNA mutation damage, but Parkin did not rescue the extent of mtDNA mutations, leading to the suggestion that Parkin compensates for mtDNA mutations by mitigating the ensuing mitochondrial proteotoxicity (Pickrell et al., 2015). Finally, ETC subunits have been shown to be differentially degraded by PINK1–Parkin, but the mechanisms of how PINK1–Parkin could select subsets of cargo remained unknown (Vincow et al., 2013). We now show that PINK1 and Parkin selectively recognize and reduce mitochondrial proteotoxicity and explore how protein aggregates are eliminated.

Drp1 was thought to be essential for mitophagy in mammalian cells to fit elongated mitochondria into nascent autophagosomes (Tanaka et al., 2010; Gomes et al., 2011; Rambold et al., 2011; Kageyama et al., 2014) or to segregate damaged components from the healthy mitochondrial network (Twig et al., 2008). However, recent work indicates that some forms of mitophagy are Drp1 independent (Murakawa et al., 2015; Yamashita et al., 2016). Similarly, one study in yeast found that inhibition of Dnm1 blocks mitophagy (Kanki et al., 2009a), whereas others have found no role for Dnm1 in regulating the rate of mitophagy (Mendl et al., 2011; Yamashita et al., 2016). In mammalian cells, the predicted necessity of small mitochondria for engulfment is not supported by electron microscope images of multiple nascent autophagosomal membranes engulfing large mitochondrial aggregates (Yoshii et al., 2011) or the capacity of autophagosomes to engulf micrometer-diameter beads (Kobayashi et al., 2010). We report in this study that, although Drp1 does mediate fission upon actinonin- and ΔOTC-induced proteotoxic stress, it is not required for mitophagy. These results contrast with our prior study that inhibiting Drp1 reduced mitophagy (Tanaka et al., 2010), where the 24-h m-chlorophenylhydrazone treatment without mitigating cell death may have skewed the results in the surviving population of cells. In this study, we show that after only 3 h of OA, by measuring cells expressing mito-Keima by flow cytometry analysis, that loss of Drp1 enhances mitophagy.

Parkin was observed to accumulate with LC3 in foci on mitochondria in neurons with a high mtDNA mutation burden (Hämäläinen et al., 2013), and after photodamage, Parkin and LC3 have been observed to colocalize on damaged mitochondrial subdomains before fragmentation from the intact network (Kim and Lemasters, 2011; Yang and Yang, 2013). However, direct visualization of damaged cargo being sequestered and degraded in mitochondrial subdomains has been lacking. We have now visualized misfolded mitochondrial matrix–localized protein aggregates being segregated into mitochondrial subdomains and incorporated into Parkin-coated fission products. Our data support a model in which Drp1 is not required for mitophagy but rather restricts PINK1–Parkin activity to specific mitochondrial subdomains by either segregating the PINK1–Parkin-positive feedback loop away from the healthy mitochondrial network and/or by removing misfolded mitochondrial proteins from the network to prevent their spreading, which may lead to wholesale loss of mitochondrial function and membrane potential perturbations (Fig. 8 H). This is consistent with work indicating that individual mitochondrial proteins have different autophagy-mediated turnover rates and that some mitochondrial protein half-lives, including electron transport chain subunits, are modulated specifically by PINK1–Parkin-mediated mitophagy (Vincow et al., 2013). Also in yeast, segregation of mitochondrial components occurs, and selective mitophagy functions under physiological conditions (Abeliovich et al., 2013; Hughes et al., 2016).

Chemical uncouplers, inhibition of mitochondrial fusion, and electron transport chain inhibitors are well established to activate PINK1–Parkin-mediated mitophagy by depolarizing the inner membrane (Youle and van der Bliek, 2012). As PINK1 requires membrane potential for import and degradation, loss of membrane potential shunts PINK1 from proteolytic cleavage by presenilins-associated rhomboid-like (PARL) protein at the inner membrane, causing PINK1 to accumulate on the outer mitochondrial membrane, where it activates Parkin in the cytosol (Jin et al., 2010; Meissner et al., 2011). ΔOTC activates PINK1–Parkin without depolarization (Jin and Youle, 2013), indicating that proteotoxicity has a novel and unknown mode in inhibiting PINK1 proteolysis by PARL. We show that this mechanism functions locally to promote focal accumulation of PINK1, Parkin, and downstream autophagy machinery. This cytosolic signaling by PINK1 of the location of protein aggregates in the matrix may explain why PINK1 is constitutively bound to the translocase of the outer membrane (TOM) complex (Lazarou et al., 2012; Okatsu et al., 2013).

Materials and methods

Cell culture

HEK293 and HeLa cells were cultured in DMEM (Thermo Fisher Scientific) supplemented with 10% (vol/vol) FBS (Gemini Bio Products), 10 mM Hepes (Thermo Fisher Scientific), 1 mM sodium pyruvate (Thermo Fisher Scientific), 1× nonessential amino acids (Thermo Fisher Scientific), and 1× GlutaMAX (Thermo Fisher Scientific). HCT116 cells were grown in 10% (vol/vol) FBS (Gemini Bio Products), 1× nonessential amino acids (Thermo Fisher Scientific), and 1× GlutaMAX (Thermo Fisher Scientific) in McCoy's media. All cells were acquired from the ATCC. All cells were tested for mycoplasma contamination bimonthly using the PlasmoTest kit (InvivoGen). HeLa cells were validated by the Johns Hopkins Genetic Resources Core Facility fragment analysis facility using Short Tandem Repeat profiling (Lazarou et al., 2015).

Cloning and generation of stable cell lines

Tet ON: WT OTC or ΔOTC with or without Parkin were previously described (Jin and Youle, 2013). To generate stably infected cell lines, retroviruses containing pBMN-mCherry-Parkin, pBabe-PINK1-V5,

or without treatment with DOX for 48 h were labeled with TMRM (red) and imaged live. (D) HeLa cells expressing Tet ON: WT OTC and ΔOTC in the same cell expressing YFP-Parkin with or without a Drp1 KO background were treated with DOX for 48 h or 48 h with a 24- or 48-h washout of DOX and then processed for Western blot analysis. (E) Quantification of Western blots as described in D expressed as the percentage of OTC levels relative to OTC levels after 48 h DOX treatment normalized to Hsp90 levels. $n = 3$. *, $P < 0.05$; **, $P < 0.01$. Error bars indicate SD. (F) WT HCT116 or HeLa cells expressing YFP-Parkin (green) with or without a Drp1 KO background were labeled with TMRM (red) and imaged live. Bars, 10 µm. (G) Tet ON: ΔOTC-expressing cells also expressing YFP-Parkin with or without a Drp1 KO background were infected with Cell Light mito-GFP virus overnight and then treated with DOX for 48 h or 48 h with a 24-h washout of DOX and processed for Western blot analysis. (H) Model depicting the role of PINK, Parkin, and Drp1 in the selective mitophagy of protein aggregates from mitochondria.

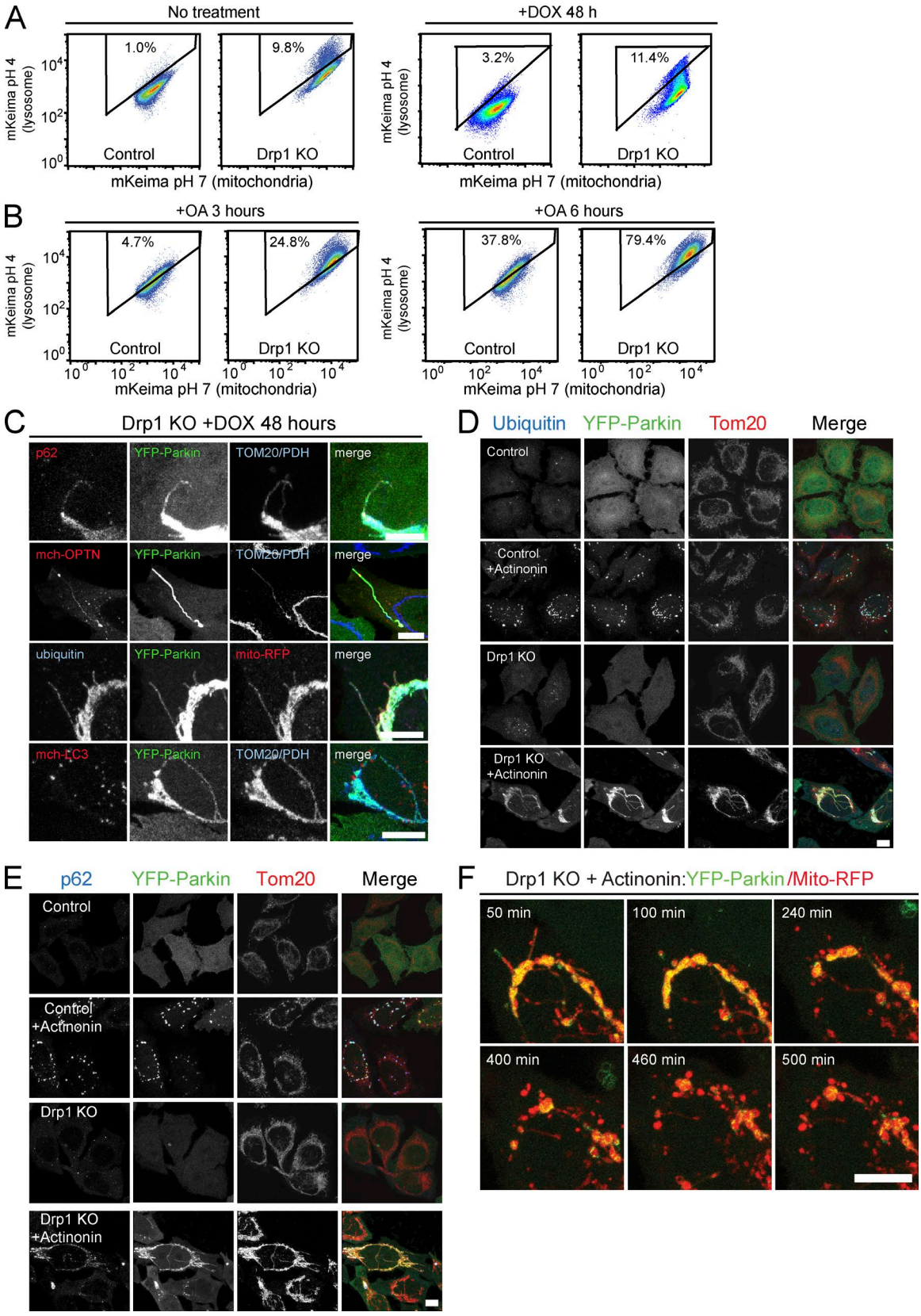

Figure 9. **Autophagy receptors are recruited to intact mitochondria in Drp1 KO cells, enhancing mitophagic flux.** (A and B) FACS-based mito-Keima assay dot plots of Tet ON: ΔOTC-expressing HeLa cells expressing YFP-Parkin with or without DOX treatment (A) or OA treatment (B) for the indicated time points with or without a Drp1 KO background. The y axis represents the fluorescence emission of mito-Keima at pH 4.0 (lysosome) versus the x axis, which indicates mito-Keima emission at pH 7.0 (mitochondria). The percentage of cells within the boxed regions are indicated. (C) Tet ON: ΔOTC-expressing Drp1 KO HeLa cells expressing YFP-Parkin (green), mCherry-optineurin, mCherry-LC3, or mito-RFP (red) were treated with DOX for 48 h and then processed for

pTRE3G-WT-OTC, or pBMN-YFP-Parkin were packaged in HEK293 cells. HeLa cells were transduced with virus for 24 h with 8 µg/ml polybrene (Sigma-Aldrich) and then selected for optimal protein expression by fluorescence cell sorting. OTC-SNAP plasmid was created using the rat OTC sequence in conjunction with Gibson Assembly ligation method (New England Biolabs, Inc.) in pcDNA3.1+.

Antibodies and dyes

The following monoclonal and polyclonal antibodies were used for Western blotting: OTC (Santa Cruz Biotechnology, Inc. or Abcam), Hsp90 (Santa Cruz Biotechnology, Inc.), Hsp60 (Enzo Life Sciences), ATG5 (Cell Signaling Technology), TOM20 (Santa Cruz Biotechnology, Inc.), Parkin (Santa Cruz Biotechnology, Inc.), PINK1 (Cell Signaling Technology), GFP (Thermo Fisher Scientific), syntaxin 17 (Novus Biologicals), and SNAP (New England Biolabs, Inc.). For immunostaining: OTC (Novus Biologicals), ubiquitin (Cell Signaling Technology), TOM20 (Santa Cruz Biotechnology, Inc.), pyruvate dehydrogenase (PDH; Abcam), p62 (Cedarlane), and PINK1 (Cell Signaling Technology) were used. Mito-RFP or mito-GFP Cell Light Virus (Thermo Fisher Scientific), 20 nM MitoTracker (Thermo Fisher Scientific), or 20 nM TMRM (Enzo Life Sciences) or 600 nM SNAP ligand–tetramethylrhodamine were used to label mitochondria according to manufacturer's protocols.

Reagents

Bafilomycin (Sigma-Aldrich) was added to 100 nM for 48-h washout time points or 200–400 nM for 24-h washout time points, and nocodazole (Sigma-Aldrich) was used at 20 nM, oligomycin (EMD Millipore) was used at 10 µM, antimycin A (Sigma-Aldrich) was used at 4 µM, and the pan-caspase inhibitor QVD (ApexBio) was used at 20 µM. DOX was used at 1 µg/ml (Sigma-Aldrich). Actinonin (Thermo Fisher Scientific) was used at 150 µM. Transfection reagents used were X-tremeGENE 9 (Roche) or polyethylenimine (Sigma-Aldrich) at 3 µl transfection reagent per 1 µg to DNA. mCherry-optineurin, GFP-LC3B, and mCherry-LC3B constructs were previously described (Lazarou et al., 2015). All constructs were sequence verified.

5′ RACE

Total RNA from HEK293 or HeLa cells were isolated with the RNeasy Plus mini kit (QIAGEN), which removes genomic DNA contamination. 5′ RACE was conducted with the GeneRacer kit containing SuperScript III RT (Invitrogen). 5 µg total RNA from HEK293 and 1 µg total RNA from HeLa cells were used for cDNA synthesis. After checking actin levels in these cDNA samples, various amounts of cDNA were used for 5′ RACE PCR to achieve equal actin levels, and the adjusted amount of cDNAs were then used for Parkin 5′ RACE PCR. Primers used were the supplied GeneRacer 5′ primer (Invitrogen) and Parkin primer set 1, 5′-GGCTCCTGACGTCTGTGCACG TAAT-3′, or Parkin primer set 2, 5′-GCGATCAGGTGCAAAGCTACT GATGT-3′, and β-actin, 5′-TGACAGGATGCAGAAGGAGAT-3′ and 5′-GCGCTCAGGAGGAGCAAT-3′.

Generation of KO lines using CRISPR-Cas9 gene editing

To generate KO cell lines, CRISPR guide RNAs were chosen that targeted an exon common to all splicing variants of the gene of interest listed in the next section. The CRISPR-Cas9 system was used to knock out ATG5, PINK1, and Drp1. Oligonucleotides (Operon) containing CRISPR target sequences were annealed and ligated into AlfII-linearized guide RNA (41824; Addgene) or pSpCas9-P2A-GFP vectors (48138; Addgene). For CRISPR-Cas9 gene editing, HeLa cells were transfected with the guide RNA constructs hCAS9 (41815; Addgene) and pEGFP-C1 (Takara Bio Inc.) or mCherry-N1 or with the all-in-one pSpCas9-P2A-GFP vector. 2 d after transfection, GFP-positive cells were sorted by FACS and plated in 96-well plates. Single colonies were expanded into 24-well plates before screening for depletion of the targeted gene product by Western blot and/or immunostaining.

CRISPR-Cas9 guide RNAs

Drp1 exon 1, 5′-GCTAGAAAGCCTGGTGGGGA-3′; PINK1 exon 1, 5′-GGAAGAAGCGGAGACGGTT-3′, and PINK1 exon 7, CRISPR 5′-TCAATCCCTTCTACGGCCA-3′; Atg5 exon 3, 5′-ATCAAGTTC AGCTCTTCCT-3′; syntaxin 17 exon 3, 5′-ACAAATATCTCCACA ATAGA-3′ and 5′-GTAGATACTGAATTATCTAT-3′.

RNAi-mediated knockdown

RNAi reagents were from GE Healthcare. RNAi was used at 20 nM with the RNAiMax (Thermo Fisher Scientific) transfection protocol. RNAi sequences were: syntaxin 17 #1 = Smartpool: L-020965-01-0005; syntaxin 17 #2 = ON-TARGET-plus Human STX17: 5′-CGAUCCAAU AUCCGAGAAA-3′; PINK1 = Smartpool: M-004030-02-0005 (GE Healthcare); mock RNAi = AllStar Negative Control siRNA (QIAGEN).

Fluorescence intensity measurements

For ΔOTC measurements in cells with or without YFP-Parkin expression, 1,000 ΔOTC-inducible cells were plated into 1,536-well dishes in 1 µg/ml DOX for 48 h. Cells were then permeabilized and blocked with 0.1% Triton X-100 and 3% goat serum in PBS for 40 min. Cells were incubated with antibodies diluted in 0.1% Triton X-100 and 3% goat blocking serum in PBS overnight at 4°C and then were rinsed with 0.1% Triton X-100 in PBS and incubated with the appropriate fluorescent secondary antibodies (Thermo Fisher Scientific) for 1 h at room temperature. Cells were washed three times for 5 min each with 0.1% Triton X-100 in PBS and imaged on an Acumen High Content Imager (TTP Labtech).

Immunoblotting

Cells were lysed in 1× LDS sample buffer (Thermo Fisher Scientific) supplemented with 150 mM DTT (Sigma-Aldrich) and heated to 99°C with shaking for 10 min. 25–50 µg of protein per sample was separated on 4–12% Bis-Tris gels (Thermo Fisher Scientific) according to the manufacturer's instructions and then was transferred to nitrocellulose membranes and immunoblotted using antibodies diluted in 1% BSA in PBS–Tween-20 overnight. It was then washed in PBS–Tween-20 and incubated with HRP-conjugated secondary antibodies in 5% milk in PBS–Tween-20 for 1 h at room temperature, and then washed again in PBS–Tween-20 and digitally imaged.

Detergent-insoluble fractionation

After a wash in PBS, cells were scraped into lysis buffer (20 mM Tris, pH 7.5, 150 mM NaCl, 10 mM EDTA, pH 8.0, and 1% Triton X-100). The cells were disrupted by pipetting up and down 10 times and then were placed on ice for 15 min. Cells were then centrifuged at ∼13,000 *g* for 10 min at 4°C and processed for Western blot analysis.

indirect immunofluorescence with an antibody to TOM20, PDH, ubiquitin (blue), or p62 (red). Each row represents a different cell. (D and E) Control or Drp1 KO HeLa cells were treated with actinonin for 6 h, fixed, and stained with an antibody to TOM20 (red) and ubiquitin (D) or p62 (blue; E). (F) Drp1 KO HeLa cells expressing YFP-Parkin (green) and mito-RFP (red) were treated with actinonin for 6 h and imaged live for the indicated times. Bars, 10 µm.

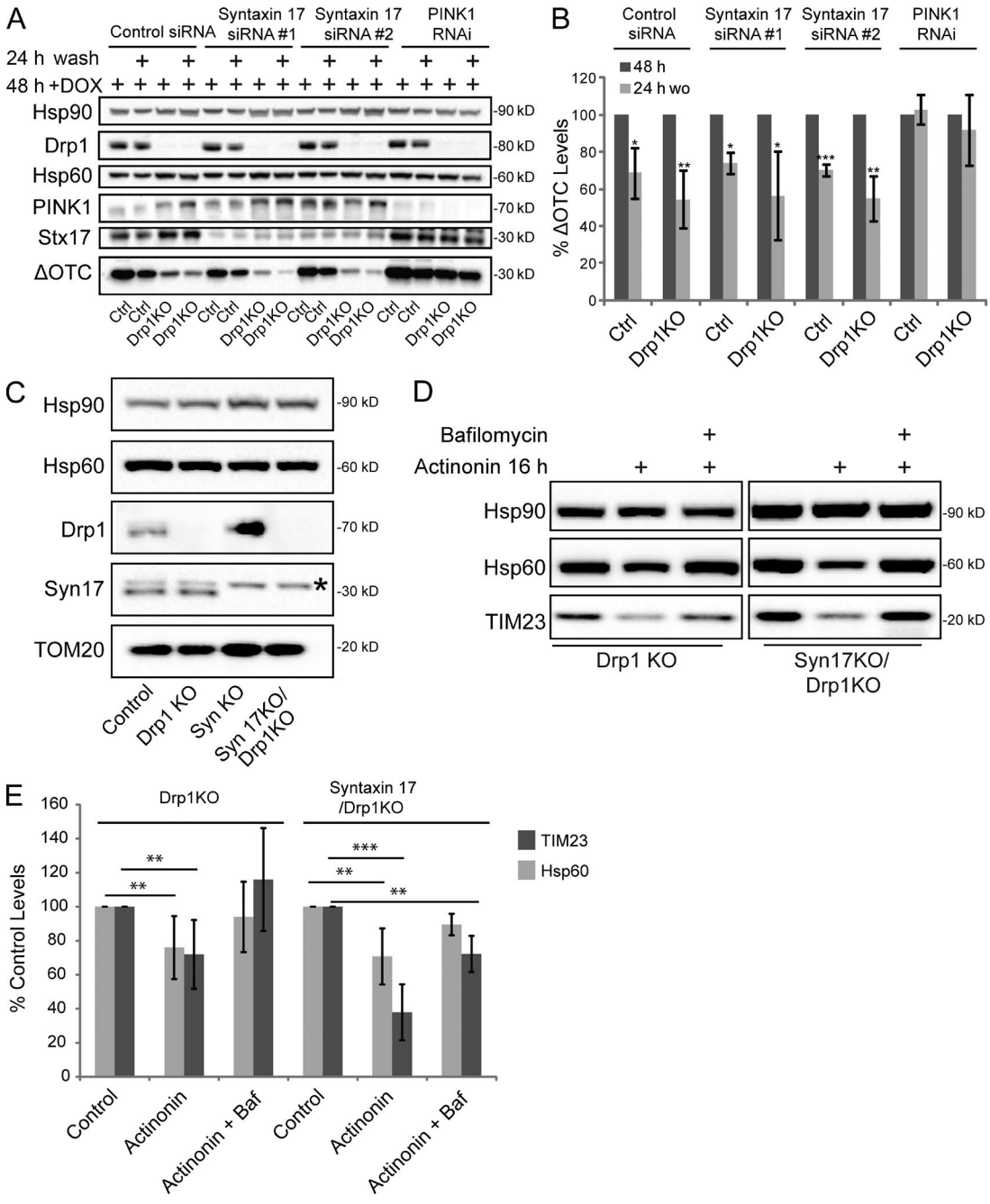

Figure 10. **MDVs are not essential for misfolded protein clearance from mitochondria.** (A) Tet ON: ΔOTC-expressing HeLa cells also expressing YFP-Parkin with or without a Drp1 KO background were treated with 20 nM control, *syntaxin 17*, or *pink1* RNAi for 24 h and then treated with DOX for 48 h or 48 h with a 24-h washout of DOX, and cells were processed for Western blot. (B) Quantification of Western blots as described in A expressed as the percentage of ΔOTC levels relative to ΔOTC levels after 48 h DOX treatment normalized to Hsp90 levels. $n \geq 3$. (C) HeLa cells expressing YFP-Parkin with or without a Drp1 KO background and with or without a syntaxin 17 KO background were processed for Western blot analysis. The asterisk indicates a nonspecific band. (D) HeLa cells expressing YFP-Parkin with a Drp1 KO background and with or without a syntaxin 17 KO background were treated with actinonin for 16 h with and without 400 nM bafilomycin treatment and then were processed for Western blot analysis. (E) Quantification of Western blots as described in D expressed as the percentage of control TIM23 or Hsp60 levels normalized to Hsp90 levels. $n \geq 3$. *, $P < 0.05$; **, $P < 0.01$; ***, $P < 0.001$. Error bars indicate SD.

Immunofluorescence microscopy

HeLa cells were seeded in two-well chamber slides (Lab-Tek; Thermo Fisher Scientific) or on small glass 15-mm coverslips. After treatment with drugs, cells were rinsed in PBS and fixed for 15 min at room temperature with 4% paraformaldehyde. Cells were permeabilized, blocked for 1 h, and incubated in primary antibody in 0.1% Triton X-100 and 3% goat serum in PBS overnight at 4°C. Cells were then rinsed with 0.1% Triton X-100 in PBS and incubated with the desired secondary antibody (Thermo Fisher Scientific) for 1 h at room temperature in 0.1% Triton X-100 and 3% goat serum in PBS. Cells were washed three times for 5 min each with 0.1% Triton X-100 in PBS with a final wash of PBS. Cells were imaged using a Plan Apochromat 63× 1.4 oil differential interference contrast objective on an LSM 510, 780, or 880 microscope running Zen software (ZEISS). For live imaging,

four image slices were collected through the z plane encompassing the majority of the cell thickness. Image analysis was performed in ImageJ (National Institutes of Health) or Zen. For quantification of mitochondrial fragmentation, cells were imaged through their entire z plane, 3D images were created and blinded, and then the fragmentation state of the mitochondria was manually scored. Superresolution imaging was conducted on an LSM 880 with Airyscan detection (ZEISS). Airyscan images were processed automatically in Zen. Alexa Fluor dyes 647, 555, 488, and 405 (Thermo Fisher Scientific) were used for all immunostaining experiments. Videos 6 and 7 were processed using the ImageJ Nonlocal Means Denoising plugin with auto-sigma factor determination and a smoothing factor of 1.

YFP-Parkin colocalization with optineurin, LC3, Drp1, and ΔOTC

Cells were transfected with mCherry-optineurin or mCherry-LC3, treated with DOX or Actinonin (Figs. 3, 4, and 9) and imaged as described in the previous section. For analysis of Drp1 and ΔOTC colocalization (Figs. 7 and S5 F), cells were fixed and stained as described in the previous section. Cells were imaged through their entire z plane using an Apochromat 63× oil differential interference contrast objective on an LSM 780 or 880. Images were analyzed and blinded to the mCherry, ΔOTC, or Drp1 channel for YFP-Parkin foci. Once identified, the mCherry or ΔOTC channel was revealed to determine whether the two signals overlapped. Only cells in which both the mCherry or ΔOTC and YFP-Parkin signal were both detectable were included.

Mito-mKeima mitophagy assay

Mito-mKeima (a gift from A. Miyawaki, Japan Science and Technology Agency, Tokyo, Japan) was cloned into a pCHAC-MCS-1-IRES-MCS2 vector (Allele Biotechnology). Cells were infected with a retrovirus harboring the mito-mKeima vector, grown for ≥3 d, and plated in 1 µg/ml DOX for 48 h. Before flow cytometry analysis, a subset of untreated control cells were treated with OA A for 3 or 6 h. Cells were labeled with DAPI (1 µg/ml) and analyzed on a FACS Aria II (BD).

Live imaging

Cells were plated in Lab-Tek two-chamber imaging dishes (Thermo Fisher Scientific), transfected with GFP-LC3 or ΔOTC-SNAP, treated with DOX for 48 h, and treated with Cell Light mito-RFP (Thermo Fisher Scientific), MitoTracker dye (Thermo Fisher Scientific), or TMRM (Enzo Life Sciences), and then imaged live on an LSM 780 with a controlled CO_2/heating chamber. Quantification of live imaging data was done blinded.

Statistical calculations

Unless otherwise indicated, data from three or more independent experiments were analyzed using an unpaired Student's *t* test to assess significance. All error bars are expressed as SD. For all experiments, n = number of independent experiments, and N = the number of cells measured in each experiment. For FACS analysis, ANOVA was used to determine significance. For all experiments, *, $P < 0.05$; **, $P < 0.01$; ***, $P < 0.001$.

Online supplemental material

Fig. S1 examines the role of Parkin in enhancing the clearance of ΔOTC from mitochondria. Fig. S2 confirms the specificity of PINK1–Parkin-mediated clearance of ΔOTC using independent CRISPR lines as well as several control experiments. Fig. S3 examines the formation of Parkin foci and mitochondrial fission in mitophagy-deficient cells. Fig. S4 examines the fate of ΔOTC aggregates and the effect of Drp1 KO on mitophagy. Fig. S5 deals with the role of Drp1 in determining the specificity of mitophagy. Videos 1, 2, 3, and 4 demonstrate the dynamic nature of mitochondrial subdomains coated in Parkin and their colocalization with LC3 before fission. Videos 5, 6, and 7 demonstrate the relationship between Drp1 and the fission of mitochondrial subdomains coated in Parkin. Videos 8, 9, and 10 demonstrate Parkin recruitment to mitochondria in Drp1 KO cells and Drp1-independent fission of Parkin-coated mitochondria.

Acknowledgments

We thank Drs. James Inglese and Patricia Dranchak for help with high-content imaging. We thank Drs. Vincent Schram (Microscopy and Imaging Core, National Institute of Child Health and Human Development) and Carolyn Smith for imaging support and the Youle laboratory members for helpful discussion and assistance. We thank Wanda Kukulski and Nick Ader for thoughtful reading of the manuscript. We thank Dragan Maric for assistance with FACS analyses.

This work was supported by the Intramural Program of the National Institute of Neurological Disorders and Stroke.

The authors declare no competing financial interests.

Author contributions: J.L. Burman designed and conducted experiments, wrote the paper, and analyzed data; R.J. Youle designed experiments, wrote the paper, and analyzed data; S. Pickles, J.N.S. Vargas, S. Sekine, C.L. Nezich, A.M. Youle, Z. Zhang, and C. Wang performed experiments and analyzed data; X. Wu performed experiments; and J.A. Hammer analyzed data.

Submitted: 15 December 2016
Revised: 7 June 2017
Accepted: 21 July 2017

References

Abeliovich, H., M. Zarei, K.T. Rigbolt, R.J. Youle, and J. Dengjel. 2013. Involvement of mitochondrial dynamics in the segregation of mitochondrial matrix proteins during stationary phase mitophagy. *Nat. Commun.* 4:2789. http://dx.doi.org/10.1038/ncomms3789

Burman, J.L., S. Yu, A.C. Poole, R.B. Decal, and L. Pallanck. 2012. Analysis of neural subtypes reveals selective mitochondrial dysfunction in dopaminergic neurons from *parkin* mutants. *Proc. Natl. Acad. Sci. USA.* 109:10438–10443. http://dx.doi.org/10.1073/pnas.1120688109

Deng, H., M.W. Dodson, H. Huang, and M. Guo. 2008. The Parkinson's disease genes *pink1* and *parkin* promote mitochondrial fission and/or inhibit fusion in *Drosophila*. *Proc. Natl. Acad. Sci. USA.* 105:14503–14508. http://dx.doi.org/10.1073/pnas.0803998105

Denison, S.R., F. Wang, N.A. Becker, B. Schüle, N. Kock, L.A. Phillips, C. Klein, and D.I. Smith. 2003. Alterations in the common fragile site gene *Parkin* in ovarian and other cancers. *Oncogene.* 22:8370–8378. http://dx.doi.org/10.1038/sj.onc.1207072

Friedman, J.R., and J. Nunnari. 2014. Mitochondrial form and function. *Nature.* 505:335–343. http://dx.doi.org/10.1038/nature12985

Gomes, L.C., G. Di Benedetto, and L. Scorrano. 2011. During autophagy mitochondria elongate, are spared from degradation and sustain cell viability. *Nat. Cell Biol.* 13:589–598. http://dx.doi.org/10.1038/ncb2220

Graef, M. 2016. A dividing matter: Drp1/Dnm1-independent mitophagy. *J. Cell Biol.* 215:599–601. http://dx.doi.org/10.1083/jcb.201611079

Hämäläinen, R.H., T. Manninen, H. Koivumäki, M. Kislin, T. Otonkoski, and A. Suomalainen. 2013. Tissue- and cell-type-specific manifestations of heteroplasmic mtDNA 3243A>G mutation in human induced pluripotent stem cell-derived disease model. *Proc. Natl. Acad. Sci. USA.* 110:E3622–E3630. http://dx.doi.org/10.1073/pnas.1311660110

Heo, J.M., A. Ordureau, J.A. Paulo, J. Rinehart, and J.W. Harper. 2015. The PINK1-PARKIN mitochondrial ubiquitylation pathway drives a program of OPTN/NDP52 recruitment and TBK1 activation to promote mitophagy. *Mol. Cell.* 60:7–20. http://dx.doi.org/10.1016/j.molcel.2015.08.016

Hughes, A.L., C.E. Hughes, K.A. Henderson, N. Yazvenko, and D.E. Gottschling. 2016. Selective sorting and destruction of mitochondrial membrane proteins in aged yeast. *eLife.* 5:e13943. http://dx.doi.org/10.7554/eLife.13943

Jin, S.M., and R.J. Youle. 2013. The accumulation of misfolded proteins in the mitochondrial matrix is sensed by PINK1 to induce PARK2/Parkin-mediated mitophagy of polarized mitochondria. *Autophagy.* 9:1750–1757. http://dx.doi.org/10.4161/auto.26122

Jin, S.M., M. Lazarou, C. Wang, L.A. Kane, D.P. Narendra, and R.J. Youle. 2010. Mitochondrial membrane potential regulates PINK1 import and proteolytic destabilization by PARL. *J. Cell Biol.* 191:933–942. http://dx.doi.org/10.1083/jcb.201008084

Kageyama, Y., M. Hoshijima, K. Seo, D. Bedja, P. Sysa-Shah, S.A. Andrabi, W. Chen, A. Höke, V.L. Dawson, T.M. Dawson, et al. 2014. Parkin-independent mitophagy requires Drp1 and maintains the integrity of mammalian heart and brain. *EMBO J.* 33:2798–2813. http://dx.doi.org/10.15252/embj.201488658

Kanki, T., K. Wang, M. Baba, C.R. Bartholomew, M.A. Lynch-Day, Z. Du, J. Geng, K. Mao, Z. Yang, W.L. Yen, and D.J. Klionsky. 2009a. A genomic screen for yeast mutants defective in selective mitochondria autophagy. *Mol. Biol. Cell.* 20:4730–4738. http://dx.doi.org/10.1091/mbc.E09-03-0225

Katayama, H., T. Kogure, N. Mizushima, T. Yoshimori, and A. Miyawaki. 2011. A sensitive and quantitative technique for detecting autophagic events based on lysosomal delivery. *Chem. Biol.* 18:1042–1052. http://dx.doi.org/10.1016/j.chembiol.2011.05.013

Keppler, A., S. Gendreizig, T. Gronemeyer, H. Pick, H. Vogel, and K. Johnsson. 2002. A general method for the covalent labeling of fusion proteins with small molecules in vivo. *Nat. Biotechnol.* 21:86–89. http://dx.doi.org/10.1038/nbt765

Kim, I., and J.J. Lemasters. 2011. Mitophagy selectively degrades individual damaged mitochondria after photoirradiation. *Antioxid. Redox Signal.* 14:1919–1928. http://dx.doi.org/10.1089/ars.2010.3768

Kobayashi, S., T. Kojidani, H. Osakada, A. Yamamoto, T. Yoshimori, Y. Hiraoka, and T. Haraguchi. 2010. Artificial induction of autophagy around polystyrene beads in nonphagocytic cells. *Autophagy.* 6:36–45. http://dx.doi.org/10.4161/auto.6.1.10324

Lazarou, M., S.M. Jin, L.A. Kane, and R.J. Youle. 2012. Role of PINK1 binding to the TOM complex and alternate intracellular membranes in recruitment and activation of the E3 ligase Parkin. *Dev. Cell.* 22:320–333. http://dx.doi.org/10.1016/j.devcel.2011.12.014

Lazarou, M., D.A. Sliter, L.A. Kane, S.A. Sarraf, C. Wang, J.L. Burman, D.P. Sideris, A.I. Fogel, and R.J. Youle. 2015. The ubiquitin kinase PINK1 recruits autophagy receptors to induce mitophagy. *Nature.* 524:309–314. http://dx.doi.org/10.1038/nature14893

Lee, J.E., L.M. Westrate, H. Wu, C. Page, and G.K. Voeltz. 2016. Multiple dynamin family members collaborate to drive mitochondrial division. *Nature.* 540:139–143. http://dx.doi.org/10.1038/nature20555

Lin, Y.F., A.M. Schulz, M.W. Pellegrino, Y. Lu, S. Shaham, and C.M. Haynes. 2016. Maintenance and propagation of a deleterious mitochondrial genome by the mitochondrial unfolded protein response. *Nature.* 533:416–419. http://dx.doi.org/10.1038/nature17989

McLelland, G.L., S.A. Lee, H.M. McBride, and E.A. Fon. 2016. Syntaxin-17 delivers PINK1/parkin-dependent mitochondrial vesicles to the endolysosomal system. *J. Cell Biol.* 214:275–291. http://dx.doi.org/10.1083/jcb.201603105

Meissner, C., H. Lorenz, A. Weihofen, D.J. Selkoe, and M.K. Lemberg. 2011. The mitochondrial intramembrane protease PARL cleaves human Pink1 to regulate Pink1 trafficking. *J. Neurochem.* 117:856–867. http://dx.doi.org/10.1111/j.1471-4159.2011.07253.x

Mendl, N., A. Occhipinti, M. Müller, P. Wild, I. Dikic, and A.S. Reichert. 2011. Mitophagy in yeast is independent of mitochondrial fission and requires the stress response gene *WHI2*. *J. Cell Sci.* 124:1339–1350. http://dx.doi.org/10.1242/jcs.076406

Murakawa, T., O. Yamaguchi, A. Hashimoto, S. Hikoso, T. Takeda, T. Oka, H. Yasui, H. Ueda, Y. Akazawa, H. Nakayama, et al. 2015. Bcl-2-like protein 13 is a mammalian Atg32 homologue that mediates mitophagy and mitochondrial fragmentation. *Nat. Commun.* 6:7527. http://dx.doi.org/10.1038/ncomms8527

Narendra, D., A. Tanaka, D.F. Suen, and R.J. Youle. 2008. Parkin is recruited selectively to impaired mitochondria and promotes their autophagy. *J. Cell Biol.* 183:795–803. http://dx.doi.org/10.1083/jcb.200809125

Nunnari, J., and A. Suomalainen. 2012. Mitochondria: In sickness and in health. *Cell.* 148:1145–1159. http://dx.doi.org/10.1016/j.cell.2012.02.035

Okatsu, K., M. Uno, F. Koyano, E. Go, M. Kimura, T. Oka, K. Tanaka, and N. Matsuda. 2013. A dimeric PINK1-containing complex on depolarized mitochondria stimulates Parkin recruitment. *J. Biol. Chem.* 288:36372–36384. http://dx.doi.org/10.1074/jbc.M113.509653

Pickrell, A.M., and R.J. Youle. 2015. The roles of PINK1, parkin, and mitochondrial fidelity in Parkinson's disease. *Neuron.* 85:257–273. http://dx.doi.org/10.1016/j.neuron.2014.12.007

Pickrell, A.M., C.H. Huang, S.R. Kennedy, A. Ordureau, D.P. Sideris, J.G. Hoekstra, J.W. Harper, and R.J. Youle. 2015. Endogenous Parkin preserves dopaminergic substantia Nigral neurons following mitochondrial DNA mutagenic stress. *Neuron.* 87:371–381. http://dx.doi.org/10.1016/j.neuron.2015.06.034

Poole, A.C., R.E. Thomas, L.A. Andrews, H.M. McBride, A.J. Whitworth, and L.J. Pallanck. 2008. The PINK1/Parkin pathway regulates mitochondrial morphology. *Proc. Natl. Acad. Sci. USA.* 105:1638–1643. http://dx.doi.org/10.1073/pnas.0709336105

Rambold, A.S., B. Kostelecky, N. Elia, and J. Lippincott-Schwartz. 2011. Tubular network formation protects mitochondria from autophagosomal degradation during nutrient starvation. *Proc. Natl. Acad. Sci. USA.* 108:10190–10195. http://dx.doi.org/10.1073/pnas.1107402108

Richter, U., T. Lahtinen, P. Marttinen, M. Myöhänen, D. Greco, G. Cannino, H.T. Jacobs, N. Lietzén, T.A. Nyman, and B.J. Battersby. 2013. A mitochondrial ribosomal and RNA decay pathway blocks cell proliferation. *Curr. Biol.* 23:535–541. http://dx.doi.org/10.1016/j.cub.2013.02.019

Roy, M., K. Itoh, M. Iijima, and H. Sesaki. 2016. Parkin suppresses Drp1-independent mitochondrial division. *Biochem. Biophys. Res. Commun.* 475:283–288. http://dx.doi.org/10.1016/j.bbrc.2016.05.038

Smirnova, E., L. Griparic, D.L. Shurland, and A.M. van der Bliek. 2001. Dynamin-related protein Drp1 is required for mitochondrial division in mammalian cells. *Mol. Biol. Cell.* 12:2245–2256. http://dx.doi.org/10.1091/mbc.12.8.2245

Song, M., K. Mihara, Y. Chen, L. Scorrano, and G.W. Dorn II. 2015. Mitochondrial fission and fusion factors reciprocally orchestrate mitophagic culling in mouse hearts and cultured fibroblasts. *Cell Metab.* 21:273–285. http://dx.doi.org/10.1016/j.cmet.2014.12.011

Soubannier, V., G.L. McLelland, R. Zunino, E. Braschi, P. Rippstein, E.A. Fon, and H.M. McBride. 2012. A vesicular transport pathway shuttles cargo from mitochondria to lysosomes. *Curr. Biol.* 22:135–141. http://dx.doi.org/10.1016/j.cub.2011.11.057

Tanaka, A., M.M. Cleland, S. Xu, D.P. Narendra, D.F. Suen, M. Karbowski, and R.J. Youle. 2010. Proteasome and p97 mediate mitophagy and degradation of mitofusins induced by Parkin. *J. Cell Biol.* 191:1367–1380. http://dx.doi.org/10.1083/jcb.201007013

Twig, G., A. Elorza, A.J. Molina, H. Mohamed, J.D. Wikstrom, G. Walzer, L. Stiles, S.E. Haigh, S. Katz, G. Las, et al. 2008. Fission and selective fusion govern mitochondrial segregation and elimination by autophagy. *EMBO J.* 27:433–446. http://dx.doi.org/10.1038/sj.emboj.7601963

Vincow, E.S., G. Merrihew, R.E. Thomas, N.J. Shulman, R.P. Beyer, M.J. MacCoss, and L.J. Pallanck. 2013. The PINK1–Parkin pathway promotes both mitophagy and selective respiratory chain turnover in vivo. *Proc. Natl. Acad. Sci. USA.* 110:6400–6405. http://dx.doi.org/10.1073/pnas.1221132110

Wong, Y.C., and E.L. Holzbaur. 2014. Optineurin is an autophagy receptor for damaged mitochondria in parkin-mediated mitophagy that is disrupted by an ALS-linked mutation. *Proc. Natl. Acad. Sci. USA.* 111:E4439–E4448. http://dx.doi.org/10.1073/pnas.1405752111

Yamashita, S.I., X. Jin, K. Furukawa, M. Hamasaki, A. Nezu, H. Otera, T. Saigusa, T. Yoshimori, Y. Sakai, K. Mihara, and T. Kanki. 2016. Mitochondrial division occurs concurrently with autophagosome formation but independently of Drp1 during mitophagy. *J. Cell Biol.* 215:649–665. http://dx.doi.org/10.1083/jcb.201605093

Yang, J.Y., and W.Y. Yang. 2013. Bit-by-bit autophagic removal of parkin-labelled mitochondria. *Nat. Commun.* 4:2428. http://dx.doi.org/10.1038/ncomms3428

Yoshii, S.R., C. Kishi, N. Ishihara, and N. Mizushima. 2011. Parkin mediates proteasome-dependent protein degradation and rupture of the outer mitochondrial membrane. *J. Biol. Chem.* 286:19630–19640. http://dx.doi.org/10.1074/jbc.M110.209338

Youle, R.J., and A.M. van der Bliek. 2012. Mitochondrial fission, fusion, and stress. *Science.* 337:1062–1065. http://dx.doi.org/10.1126/science.1219855

Zhao, Q., J. Wang, I.V. Levichkin, S. Stasinopoulos, M.T. Ryan, and N.J. Hoogenraad. 2002. A mitochondrial specific stress response in mammalian cells. *EMBO J.* 21:4411–4419. http://dx.doi.org/10.1093/emboj/cdf445